

Measurement of Size-specific Filtration Efficiency and Pressure Drop through Face  
Masks

by

Solbee Seo

A thesis submitted in partial fulfillment of the requirements for the degree of

Master of Science

Department of Mechanical Engineering  
University of Alberta

© Solbee Seo, 2023

## **Abstract**

It is common for face masks to be used in conditions that mask manufacturers did not intend, such as multiple donning of masks during supply shortage, but the mask performance in varying usage conditions are typically not regulated and assumed beneficial without the quantification of the actual mask performance. The objective of this thesis was to examine the effects of the following two common usage conditions which may influence parameters that are critical to filtration: 1) moist heat incubation decontamination of respirators for reuse and 2) lower face velocity from school-aged children breathing through woven and nonwoven masks. The results were supported by measuring size-specific filtration efficiency (FE) and pressure drops of different masks, using a custom experiment set-up with an Electrical Low Pressure Impactor.

When mask supply was limited due to high demand, various decontamination methods were used for reuse of masks, and moist heat incubation was deemed one of the least damaging methods. The first part of the thesis exposed two different respirator brands to multiple cycles of high temperature and humidity to emulate repeated moist heat incubation. The moist heat incubation method was found negligibly damaging to a certified N95 but significantly decreased the other respirator's FE, while both respirators' pressure drops were not affected. Scanning electron microscopy images of the respirators confirmed minimal physical degradation on both respirators after the decontamination. The shift of the most penetrating particle size from 0.3  $\mu\text{m}$  to 0.5  $\mu\text{m}$  suggested that the electrostatic effect may have been reduced and consequently decreased FE.

Mask performance when used by younger populations has been presumed to be similar to adults, however, children's vulnerability to a wider range of particle sizes and lower face velocity compelled the quantifications of children's masks at a face velocity representative of children.

When lower face velocity expected for school-aged children was used, the study confirmed the single fiber filtration theory in which lower face velocity increases FE and decreases pressure drop in general, but it did not yield a statistically significant increase in FE for woven masks beyond 0.05  $\mu\text{m}$ .

The results from this thesis demonstrate that a more inclusive FE test with test particle sizes ranging from nanometers to microns as well as different flow rates can reveal the unforeseen flaws of modifications to masks. The decrease in FE from repetitive moist heat incubation decontaminations was quantified, and the range of particle sizes in which the decrease occurred suggested the potential decay of the electrostatic filtration effect. Furthermore, compared to nonwoven masks, woven masks lacked protection against submicron-sized particles at both face velocities representative of adults and school-aged children. Coupled with future undertakings including examination of mask fit and intrinsic mask material properties, the results from this thesis and similar future studies can assist in developing masks resilient to changes in external factors like face velocity and user environment.

## **Preface**

The experimental apparatus used in Chapter 3 and 4 was modified by C. A. Ruzycki, H. Wang, W. H. Finlay, A. R. Martin, and myself to utilize NaCl isotonic solution and fit cut-out masks in an airtight manner, based on the previous aerosol exposure plenums built by Golshahi et al. (Golshahi et al., 2011) and Tavernini et al. (Tavernini et al., 2018).

Chapter 3 of this thesis has been published as the following: Seo, S., Ruzycki, C. A., Johnson, B., Wang, H., Vehring, R., Romanyk, D., Finlay, W. H., & Martin, A. R. (2022). Size-Specific Filtration Performance of N95 Respirators after Decontamination by Moist Heat Incubation. *Journal of Aerosol Medicine and Pulmonary Drug Delivery*, 35(1), 41–49. <https://doi.org/10.1089/jamp.2021.0002>. Permission was granted by the publisher for republishing it in the thesis. C. A. Ruzycki, S. Tavernini, H. Wang, W. H. Finlay, and A. R. Martin designed the experiment set-up; I was responsible for the data collection, data analysis, and interpretation with the assistance of B. Johnson for filtration tests and M. Gomez for SEM images. All authors contributed to the revision of the article.

Chapter 4 was a co-authored manuscript for which I was the primary author and will be submitted for publication in a scientific journal. I was responsible for modifying the test set-up previously used in Chapter 3 and for the data collection as well as data analysis and interpretation. All authors contributed to the revision of the article. The co-authors who will be included in the manuscript are C. A. Ruzycki, W. H. Finlay, D. L. Romanyk, and A. R. Martin.

The drafting of this manuscript was my responsibility with significant editorial support, direction, and contributions from D. L. Romanyk and A. R. Martin.

## **Acknowledgments**

I would first like to thank my supervisors, Dr. Martin and Dr. Romanyk, for an opportunity to work on a meaningful project during the COVID-19 pandemic and for their guidance, support, and expertise throughout the project. I am grateful that I had opportunity to learn about aerosol science, and thanks to this project and Dr. Martin and Dr. Romanyk's advice, I also grew professionally as a researcher/engineer. Their passion and expertise deeply inspired me and preserved my respect and faith in the scientific community that strives for the greater good of humanity. Thank you both for all the virtual meetings, emails, and hours that you dedicated to this project. Because you encouraged me to be more critical, independent, creative, and communicative, this project was able to come to fruition and will be one of my most meaningful achievements.

I would also like to thank the past and present members of Aerosol Research Lab and Orthodontic Biomechanics Testing and Development Group for their technical and mental support as well as free coffee/tea/chocolate. Even with the limited interactions during the pandemic, all the members inspired me with their passion and made me feel welcome in the community. Furthermore, I thank past and present members of Particle Engineering Lab for sharing various lab equipment and helping me set up, as well as Dr. Reinhard Vehring and Dr. Warren Finlay for providing valuable comments and critiques.

I would like to acknowledge my friends and family for their interest in the project and support. Thanks to their encouragement, I was able to keep showing up, look at problems from different perspectives, and learn something new every day.

Finally, I would like to acknowledge the financial support from the Natural Sciences and Engineering Research Council of Canada (NSERC). Their generous financial support made the work in this thesis possible.

Solbee Seo

December 14<sup>th</sup>, 2022

Edmonton, AB, Canada

## Table of Contents

Abstract.....	ii
Preface.....	iv
Acknowledgments.....	v
Table of Contents.....	vii
List of Tables.....	ix
List of Figures.....	x
List of Symbols.....	xi
Chapter 1: Introduction.....	1
1.1.    Motivation.....	1
1.2.    Objective.....	1
1.3.    Thesis Organization.....	2
Chapter 2: Background.....	4
2.1.    Theoretical Approach to Filtration Efficiency Through Single Fiber Filtration Theory and Pressure Drop through Davies' Equation.....	4
2.2.    Intrinsic Differences Among Face Masks.....	10
2.3.    Measurement of Mask Performance: Filtration Efficiency and Pressure Drop.....	13
Chapter 3: Effect of Moist Heat Incubation on Filtration Efficiency of High-Performance Masks .....	19
3.1.    Introduction.....	19

3.2.	Method.....	24
3.3.	Results .....	28
3.4.	Discussion.....	30
3.5.	Conclusion.....	35
Chapter 4: Effect of Children’s Expected Face Velocity on Filtration Efficiency of Children’s Masks .....		
		36
4.1.	Introduction .....	36
4.2.	Method.....	38
4.3.	Results .....	45
4.4.	Discussion.....	55
4.5.	Conclusion.....	59
Chapter 5: Conclusion.....		
		60
5.1.	Summary.....	60
5.2.	Future Work.....	61
Works Cited .....		
		63



## List of Tables

Table 2 - 1 Five mechanisms of filtration according to single fiber filtration theory. Image adapted from (Hinds, 1999).....	8
Table 2 - 2 Comparisons of different methods to test FE and pressure drop of masks (FDA, 2004; Fit, n.d.; Gb-, 2006; Rengasamy et al., 2017; Scheepers et al., 2021; Science 3M, 2020; The US Public Health Service, 2012) .....	15
Table 2 - 3 Comparison between ELPI and ELPI+ .....	18
Table 3 - 1 Comparisons between current and previous studies on the effects of moist heat incubation (MHI) on respirators .....	22
Table 3 - 2 Filtration efficiency (FE)at the most penetrating particle size (MPPS) before and after ten cycles of moist heat incubation (MHI) .....	29
Table 3 - 3 Pressure drops across commercial N95s before and after ten cycles of moist heat incubation (MHI) .....	30
Table 4 - 1 Masks specifications.....	40
Table 4 - 2 Children's inhalation rates during high workload from previous literature.....	42
Table 4 - 3 Pressure drops and relative changes in filter quality for different face velocities.....	53
Table 4 - 4 p-values from Holm test (95% confidence interval) .....	53

## List of Figures

Figure 3 - 1 Experimental setup used to quantify filtration efficiencies across a range of particle sizes and pressure drops. A comparison of number concentrations measured by Electric Low Pressure Impactor in the blank and filter lines drawing from well-mixed test particles in a large plenum allowed quantification of filtration efficiencies across various particle sizes. ....	26
Figure 3 - 2 Filtration efficiencies from commercial N95s before and after ten cycles of moist heat incubation (MHI). Grey area indicates typical NIOSH test particle sizes (aerodynamic diameter of 0.06 $\mu\text{m}$ to 0.21 $\mu\text{m}$ ). For clarity, only negative error bars are depicted. ....	29
Figure 3 - 3 SEM images of commercial N95 respirators before and after ten cycles of moist heat incubation (MHI). ....	31
Figure 4 - 1 Experiment set-up to measure pressure drop and size-specific material filtration efficiency.....	43
Figure 4 - 2 Size-specific filtration efficiencies of the five mask types at two different face velocities .....	46

## List of Symbols

A	Cross Sectional Area
$\alpha$	Filter Packing Density
C	Concentration
$C_c$	Cunningham Correction Factor
D	Particle Diffusion Coefficient
$d_f$	Fiber Diameter
$d_p$	Particle Diameter
$\Delta P$	Pressure Drop
$\epsilon_f$	Relative Permittivity of Fiber
$\epsilon_0$	Permittivity of Vacuum
FE	Filter Efficiency
g	Gravitational Acceleration
Ku	Kuwabara Hydrodynamic Factor
m	Mass Concentration
$\mu$	Dynamic Viscosity
Pe	Peclet Number
Q	Volumetric Flow Rate
q	Charge of Particle
$q_f$	Filter Quality
$\rho_g$	Density of Gas
$\rho_p$	Density of Particle
Re	Reynolds Number
Stk	Stokes Number
t	Thickness
U	Face Velocity

## Chapter 1 Introduction

### 1.1. Motivation

Face masks have been widely used for protection from germs since the emergence of germ theory, which, in addition to advocating the elimination of germs by antiseptic, stresses the importance of stopping them from entering the body (Strasser & Schlich, 2020). Recently, research on the performance of face masks has surged during aerosol-transmitted pandemics such as SARS, H1N1, and COVID-19 (Ahmad et al., 2021). The protective capacity of masks is largely limited by available materials and manufacturing technology; hence, instead of being forward-engineered with initial specifications, the performance of masks is often reverse-engineered, i.e., it is investigated only after the masks have been introduced. Furthermore, modifications to masks, including decontamination procedures and the donning of multiple masks, have been improvised to mitigate supply shortages, decrease discomfort caused by prolonged use, or increase the degree of protection afforded. This ad hoc approach offers flexibility in the protection of healthcare workers and the general public, but it also introduces ambiguities needing clarification. To optimize the manufacturing processes for improved filter specification, performance, and user experience, it is important to continuously evaluate the filtration efficiency of masks in conditions closest to realistic exposure.

### 1.2. Objective

The objective of this thesis was to contribute to the effort of quantifying the filtration efficiencies and pressure drops of existing masks against test particles ranging from nanometer ( $0.001 \mu\text{m} < d_p < 0.01 \mu\text{m}$ ) to submicron ( $0.01 \mu\text{m} < d_p < 1 \mu\text{m}$ ) diameters. Ultimately, it is to resolve ambiguities in the filtration efficiencies in usage conditions that are different from standard testing environments used by regulators such as the United States' National Institute for

Occupational Safety and Health. This thesis focused on the following two usage conditions which are commonly implemented but suspected to affect crucial parameters of filtration including electrostatic effect and face velocity:

- i. Repeated cycles of decontamination through moist heat incubation for reuse of masks
- ii. Different flow rates that were expected for different populations such as school-aged children versus adults

It should be noted that the manufacture of masks did not fall within the scope of this thesis; rather, only commercially available masks were used in the experiments presented in the following chapters, and mask fit was not considered.

### 1.3. Thesis Organization

This thesis is composed of five chapters. The present chapter (1) provides the motivation for research into the filtration efficiencies of masks, the objective of this specific thesis project, and the organization of its presentation here. Chapter 2 provides background on single-fiber filtration theory, different types of masks, and typical filtration efficiency test methods from regulatory standards and other literature, all of which inform the customized filtration efficiency test set-up incorporating an ELPI. Chapter 3 examines the effect of repeated decontamination through moist heat incubation (i.e., the indirect effect of recurrent and protracted exposures to high temperature and humidity) on adult respirators' size-specific filtration efficiency. This chapter is a reformatted version of a manuscript titled "Size-Specific Filtration Performance of N95 Respirators after Decontamination by Moist Heat Incubation," published in the *Journal of Aerosol Medicine and Pulmonary Drug Delivery* in 2022. Chapter 4 examines the effect of another prominent external factor in filtration efficiency: face velocity, in the context of younger

populations' use of masks. To imitate children's minute volume flow rate, a lower face velocity was chosen for comparison with the typical minute volume flow rate for adults. This chapter is a reformatted version of a manuscript titled "Size-specific Filtration Efficiency and Pressure Drop of School-aged Children's Woven and Nonwoven Masks at Children's Minute Volume," to be submitted to a scientific journal for publication. Chapter 5 summarizes the conclusions of this thesis and suggests future work in evaluating mask performance.

## Chapter 2 Background

The following chapter provides background on the theoretical approach to filtration efficiency and pressure drop of a filter. Furthermore, the characteristics of the three main categories of masks – cloth masks, surgical masks, and disposable respirators – are summarized. The methods to evaluate mask performance that previous literature and regulators used are also discussed.

### 1.4. Theoretical Approach to Filtration Efficiency Through Single Fiber Filtration Theory and Pressure Drop through Davies' Equation

Filtration efficiency (FE) and pressure drop are essential benchmarks to determine the filters' performance, and previous literature simplified its relationship with filters' intrinsic and external factors through single fiber filtration theory and Davies' equation. FE is the fraction of particle mass or count concentration retained by the filter compared to the entering particle mass or count concentration as shown respectively in Equation 2 - 1 and Equation 2 - 2. Note that  $FE_{\text{mass}}$  equates to FE measured based on particle counts if monodisperse test particles are used (Sipkens et al., 2022). Pressure drop across the filter is caused by the resistance of air through the filter material.

$$FE_{\text{mass}} = \frac{m_{\text{in}} - m_{\text{out}}}{m_{\text{in}}} = \frac{m_{\text{filtered}}}{m_{\text{in}}} \quad \text{Equation 2 - 1}$$

$$FE = \frac{C_{\text{in}} - C_{\text{out}}}{C_{\text{in}}} = \frac{C_{\text{filtered}}}{C_{\text{in}}} \quad \text{Equation 2 - 2}$$

Where  $m$  is mass concentration (for example, in the unit of [mg per m<sup>3</sup>]); and  $C$  is count concentration (for example, in the unit of [particle counts per cm<sup>3</sup>]).

Single fiber filtration theory relates FE and external factors like particle size, assuming that intrinsic characteristics of filters such as porosity and fiber diameter are known. The basis of the theory is that the interaction between multiple particles and a filter composed of multiple fiber

threads can be represented by compounded interactions between a single aerosol and a single fiber of a filter. Let  $FE_{\text{single}}$  be a single fiber's FE per unit length of a fiber, i.e., the number of aerosols collected compared to the number of aerosols to which a single fiber is exposed. If  $FE_{\text{single}}$ , filter packing density (i.e.,  $\frac{\text{fiber volume in filter}}{\text{total volume of filter}}$ ), the total thickness of the filter, and diameter of the filter fiber are known, FE for the whole filter can be estimated by Equation 2 - 3 (Hinds, 1999). This shows that a denser (i.e., higher  $\alpha$ ), deeper (i.e. higher  $t$ ) filter with finer fibers (i.e. smaller  $d_f$ ) filter will yield higher FE.

$$FE_{\text{whole}} = 1 - \exp\left(\frac{-4 * FE_{\text{single}} * \alpha * t}{\pi * d_f}\right) \quad \text{Equation 2 - 3}$$

Where  $\alpha$  is filter packing density;  $t$  is the total thickness or depth of filter; and  $d_f$  is the diameter of a fiber.

Like single fiber filtration theory, pressure drop can also be related to a single fiber FE. Davies's equation (1973) can be derived by applying dimensional analysis to Darcy's equation on pressure drop in the laminar flow of a viscous gas through a porous bed and be rearranged as Equation 2 - 4 (Rivers & Murphy, 2000). According to Davies' equation, a more porous, shallower filter with fibers with larger diameters would yield a lower pressure drop, which is associated with ease to breathe through the filter. Notably, the two desirable outcomes – high FE and low pressure drop – require intrinsic factors that are opposing to each other, for example, smaller fiber diameter for high FE and larger fiber diameter for low pressure drop. In terms of external factors, pressure drop increases as face velocity (the flow rate through the filter divided by cross-sectional area of the filter exposed to the flow as shown in Equation 2 - 5) increases. In order to relate the effects of both FE and pressure drop simultaneously, a filter quality,  $q_f$ , can be used to represent the ratio of FE and pressure drop as shown in Equation 2 - 6 (Hinds, 1999). In short, higher FE and lower pressure drop would yield a high filter quality, which is desirable.



$$\Delta P = \frac{\left( \frac{-4 * FE_{\text{single}} * \alpha * t}{\pi * d_f} \right) * t * U * f(\alpha)}{d_f^2} \quad \text{Equation 2 - 4}$$

Where  $U$  = face velocity;  $f(\alpha) = 64 * \alpha^{1.5} (1 + 56 * \alpha^3)$  for  $0.006 < \alpha < 0.3$ .

$$U = \frac{Q}{A} \quad \text{Equation 2 - 5}$$

Where  $Q$  = the volumetric flow rate through the filter;  $A$  = cross sectional area of the filter exposed to the flow.

$$q_f = \frac{\ln\left(\frac{1}{1 - FE}\right)}{\Delta P} \quad \text{Equation 2 - 6}$$

#### 1.4.1. Five Filtration Mechanisms According to Single Fiber Theory

The single fiber theory further dictates that filtration can be achieved through five main mechanisms (Hinds, 1999), which can be simplified by equations shown in Table 2 - 1:

1. Interception
2. Gravitational Settling
3. Inertial Impaction
4. Diffusion
  - 4a. Interception of Diffusing Particles
5. Electrostatic Filtration

According to the single fiber theory (Hinds, 1999), filtration through interception occurs when a particle follows a gas streamline and is within the particle's single radius from the fiber surface. Gravitational settling occurs when a particle lands on the fiber due to gravity, which is less likely to occur when the particle is traveling fast across the fiber. Inertial impaction occurs when a particle is unable to follow a gas streamline around the fiber and continues to travel in a straight line to intersect the fiber due to inertia. Diffusion occurs when a particle impacts on to the

fiber due to the particle's random Brownian motion while travelling along the streamline. Note that diffusing particles increase the chance of intercepting the fiber, and this added filtration is referred to as the interception of diffusing particles. Lastly, electrostatic filtration occurs when a particle and the fiber are differently charged and electrostatically attract each other. The sum of the filtration contributed from each mechanism represents the overall FE as shown in Equation 2 - 7. (Hinds, 1999)

$$\begin{aligned}
 FE_{\Sigma} = & FE_{\text{Interception}} + FE_{\text{Gravitational}} + FE_{\text{Impaction}} + FE_{\text{Diffusion}} \\
 & + FE_{\text{Interception of Diffusing Particles}} + FE_{\text{Electrostatic}}
 \end{aligned}
 \tag{Equation 2 - 7}$$

The relevant equations and graphic demonstrations for each mechanism are tabulated in Table 2 - 1. Based on the theory, the only relevant external factors to FE are entering particle sizes and face velocity, and interception is not affected by face velocity. It should be noted that the contribution of the electrostatic mechanism is often challenging to quantify because the charges on the fiber and particle can easily change. Furthermore, the chance of interception, impaction, and gravitational settling increases while diffusion decreases as particle size increases, and vice versa. Because of this opposing effect in different mechanisms, it is typical to have a U-shaped pattern of FE over a range of particle sizes, i.e. higher FE at smaller and larger particle sizes and lowest FE in between.

Table 2 - 1 Five mechanisms of filtration according to single fiber filtration theory. Image adapted from (Hinds, 1999)

Filtration Mechanism	Graphical Depiction	Filtration Efficiency by Each Mechanism
Interception		$FE_{\text{Interception}} = \frac{(1 - \alpha) * R^2}{Ku * (1 + R)}$
Gravitational Settling*		$FE_{\text{Gravitational}} = G * (1 + R)$
Inertial Impaction		$FE_{\text{Impaction}} = \frac{(\text{Stk}) * J}{2 * Ku^2}$
Diffusion		$FE_{\text{Diffusion}} = 2 * Pe^{-2/3}$

Table 2 - 1 continued:

Filtration Mechanism	Graphical Depiction	Filtration Efficiency by Each Mechanism
Interception of Diffusing Particles	N/A	$FE_{\text{Intercept.of Diff.Particle}} = \frac{1.24 * R^{2/3}}{(Ku * Pe)^{1/2}}$

Electrostatic Effect**		$FE_{\text{Electrostatic}} = 1.5 * \left[ \frac{\epsilon_f - 1}{\epsilon_f + 1} * \frac{q^2}{12\pi^2 \mu U_o \epsilon_o d_p d_f^2} \right]^{1/2}$
------------------------	--	---

Where

$$R = \frac{d_p}{d_f}$$

$$Ku = f(\alpha) = -\frac{\ln \alpha}{2} - \frac{3}{4} + \alpha - \frac{\alpha^2}{4}$$

$$G = \frac{\rho_g * d_p^2 * C_c * g}{18 * \mu * U_o}$$

$$Stk = \frac{\rho_p * d_p^2 * C_c * U_o}{18 * \mu * d_f}$$

$$J = f(\alpha, R) = (29.6 - 28 * \alpha^{0.62}) * R^2 - 27.5 * R^{2.8} \text{ for } R < 0.4$$

$$Pe = \frac{d_f * U_o}{D}$$

Note:

\* The equation in this table is for the instance when the direction of gas flow and gravity are aligned; if not, the value will be negative.

\*\* Note that a fiber or particle may be charged neutral, positive, or negative as long as they are different from each other. The equation in this table is for a neutral fiber and a particle with charge, q, based on experimental measurements with glass fiber filters.

Using single fiber filtration theory, the effects of varying intrinsic and external factors can be simulated. For instance, Huang et al. simulated that if face velocity increases, filter quality is the most sensitive to changes in the velocity compared to FE; the most penetrating particle size increases for electrically charged filters and decreases for mechanical filters without electrostatic effect (Huang et al., 2013). Davies' equation and single fiber filtration theory help isolate the effects of different intrinsic factors within the filter as well as extrinsic factors, and this can help emulate realistic or worst-case environments during the performance tests and help improve FE and pressure drop in commercial masks.

### 1.5. Intrinsic Differences Among Face Masks

As shown in the single fiber filtration model, intrinsic characteristics of masks such as fiber diameter contribute to FE and pressure drops. Based on materials, manufacturing processes, fit, and regulations, commercial masks that are commonly used by the public or healthcare workers can be categorized into three groups: disposable respirators, surgical masks, and cloth masks. Disposable respirators such as N95 respirators are typically half masks made of four layers including nonwoven fabric from polypropylene and designed to be fitted for a tight seal, typically with overhead elastics. Surgical masks are usually pleated and loosely fitted to the user with ear loop elastics but similar to respirators they are composed of multiple layers with nonwoven fabric. Cloth masks can be made from various fabrics including cotton, silk, and nylon, and often come with ear loops (Ju et al., 2021). Air-supplying respirators like self-contained breathing apparatus (SCBA) and some air-purifying respirators including chemical-cartridge respirators, gas masks, and powered air-purifying respirator were not considered in this thesis because it is often economically unfavorable due to their requirement for regular maintenance and replaceable

components such as re-chargeable batteries hence it is used mostly only in industrial settings, not by the general public or healthcare workers (Ju et al., 2021; Licina & Silvers, 2021).

Cloth masks can be woven (crossing threads, which can be characterized by threads per inch), knitted (interlocking loops of fiber), or felted (compressed disorganized fibers) (Clase et al., 2020). Cloth masks can be made from various fabrics including muslin, silk, satin, and chiffon, but cotton or cotton blends with synthetic fibers like polyester, nylon, or spandex is the most common (Clase et al., 2020; Konda et al., 2020). As the majority of the cloth materials are woven (Zangmeister et al., 2020), the term “cloth masks” will be used to represent “woven masks” throughout the thesis. Cloth masks differ from each other by fabric material, thread count, number of layers, fit, design, and overall heaviness (Clase et al., 2020; Ju et al., 2021). Cotton fibers typically have fiber diameters ranging from 1 to 22  $\mu\text{m}$ , and wools can vary between 10 to 40  $\mu\text{m}$  (Zangmeister et al., 2020). Higher thread counts (greater than 100 yarns per square inch) with raised fiber texture protruding from the 2D plane are likely to lead to higher FE in cloth masks (Zangmeister et al., 2020). Cloth masks are typically preferred due to their better breathability, accessibility, and reusability (Ju et al., 2021). However, it has been shown that cloth masks’ filtration efficiencies are inferior to N95 respirators or surgical masks (Ju et al., 2021; Tcharkhtchi et al., 2021). Filtration in orderly-structured woven fabrics is limited to void spaces between yarns, while nonwoven fabrics’ homogeneous randomness throughout the material allows filtration in all surface areas (Gong & Ozgen, 2017).

Surgical masks and disposable respirators generally have better FE than cloth masks and single-use capacity. Masks at hospitals were initially made from gauze which was sanitized and reused (Rockwood, C. A., O’Donoghue, 1960). As the production of synthetic materials increased in the 1960s, gauze in the masks started to be replaced by nonwoven synthetic fibers for single-

use capacity which helped with sterility as well as lower labor cost and less management to reuse the masks (Strasser & Schlich, 2020). On the industrial side, breathing apparatus including respirators was first certified in 1919 in the United States. The use of respirators started to be further regulated through the Federal Coal Mine Health and Safety Act in 1969, from which the Occupational Safety and Health Administration (OSHA) and the National Institute of Occupational Safety and Health (NIOSH) were established in 1970. Reinforced by the tuberculosis guideline to mandate the usage of respiratory protective equipment in the 1990s, respirators used in health care started to be strictly regulated as well. Because of this backbone in the mining industry, it is notable that the filter test method tries to assess efficiency “to remove particulates of the most penetrating size regardless of the particulate composition and toxicity” (NPPTL, 2018) while the chemical composition of particles can vary in everyday life and especially health care environment and influence the degree of electrostatic FE. (Ju et al., 2021)

Surgical masks are typically 3-ply: the outermost layer is waterproof to repel fluids like droplets, the middle layer is the filter, and the innermost layer is an absorbent material that prevents droplets from the user to leak out (Chua et al., 2020). The filter component in surgical masks is nonwoven fabric, a mass of disorderly fibers bonded together through heat, chemical, or mechanical means. Often cheap polypropylene is used for material, and typically melt blow is used to manufacture the nonwoven filters. During the melt blow process, molten polymer is pushed through a die with a small orifice by blowing hot air (Chua et al., 2020), and the resulting fiber diameter ranges between 1 and 5  $\mu\text{m}$  (Adanur & Jayswal, 2020).

Respirators like N95 typically consist of three to four principal layers, which include a support layer and a filter layer which is often electret, i.e. electrically charged (Tcharkhtchi et al., 2021). One of the methods to manufacture electrets is to use electrospinning. Electrospinning is a

process in which a charged, molten polymer solution is drawn to an oppositely charged collector and attains permanent electric charges within the resulting fiber (Hutten, 2007). The mean diameter of electrospun fibers ranges from 100 nm to 500 nm, finer than melt-blown fibers (Adanur & Jayswal, 2020). Similar to the melt blow process, this type of manufacturing process creates a random array of fibers in nonwoven fabric, compared to an organized array in woven fabric (Zangmeister et al., 2020).

#### 1.6. Measurement of Mask Performance: Filtration Efficiency and Pressure Drop

FE and pressure drop of masks have been formally and informally measured by using different flow rates and test particles. The performance of masks can be tested through FE, fluid resistance, flame resistance, and differential pressure across the material (Forouzandeh et al., 2021). Note that in this thesis, only FE and differential pressure are discussed in terms of the performance of masks because fluid resistance and flame resistance depend on masks' intrinsic characteristics while the focus of the thesis is the effect of external factors. For example, fluid resistance is largely determined by polarity, viscosity surface tension, structure, and the relative hydrophobicity within the fabric (Forouzandeh et al., 2021).

Filtration efficiencies can be tested by using particulates, bacteria, or viruses as test particles. Particulates used for tests may be sodium chloride (NaCl), dioctyl phthalate (DOP), or latex (Rengasamy et al., 2017). Bacteria and viruses are also used to measure FE assuming exposure to living particles. The bacteria used for FE tests is often staphylococcus aureus with a size of 3.0  $\mu\text{m}$  (Forouzandeh et al., 2021). Viruses are not formally used for regulation but it is sometimes used to demonstrate the anti-viral effect of masks (Rengasamy et al., 2017) by groups such as Nelson Laboratories or to represent bio aerosols smaller than bacteria (Forouzandeh et al.,



2021). However, it should be noted that the parameters of the particles that directly affect FE are size, shape, and density, not the viability of the particles (Brosseau & Shaffer, 2014).

Pressure drops are related to breathability and FE hence it is regulated along with FE. It is often measured through a manometer to measure differential pressure drop across the material (Ju et al., 2021). See Table 2 - 2 for the summary of FE and pressure drop tests in formal and informal methods in different countries. Note that when the flow rate is fixed, the whole surface area of masks is exposed to the flow and may result in different face velocities amongst different mask models. Furthermore, note that instruments commonly used to conduct NIOSH certification tests employ photometers, calibrated against external mass measurements, to effectively measure  $FE_{mass}$  as shown in Equation 2 - 1 (Sipkens et al., 2022). Compared to other tests, FE test to certify NIOSH's N-series respirators such as N95 is considered one of the demanding tests as neutralized NaCl particles and relatively high flow rates tend to yield lower FE than other tests like bacterial FE test (Rengasamy et al., 2017).

Table 2 - 2 Comparisons of different methods to test FE and pressure drop of masks (3M, 2021; ChineseStandard.net, n.d.; Encycla, n.d.; FDA, 2004; Rengasamy et al., 2017; Scheepers et al., 2021; The US Public Health Service, 2012)

Country	Mask Type	Regulation Reference	Particle Type	Particle Size
The US	N95	NIOSH-42 CFR Part 84	Neutralized NaCl	$0.075 \pm 0.020 \mu\text{m}$ CMD (count median diameter) (GSD < 1.86)
	P95		Neutralized DOP particles	$0.185 \pm 0.020 \mu\text{m}$ CMD (GSD < 1.60)
	Surgical Masks	<ul style="list-style-type: none"> <li>• ASTM F2299 (PFE)</li> <li>• MIL-M- 36945C (Pressure Drop)</li> </ul>	Neutralized latex spheres	0.1 to 5.0 $\mu\text{m}$ MPS (mono- disperse aerosol)
			<ul style="list-style-type: none"> <li>• ASTM F2101 (BFE)</li> <li>• MIL-M- 36945C (Pressure Drop)</li> </ul>	Staphylo- coccus aureus bacteria
Europe	FFP2	EN 149:2001	NaCl and paraffin oil	<ul style="list-style-type: none"> <li>• 0.6 <math>\mu\text{m}</math> for NaCl</li> <li>• 0.3 <math>\mu\text{m}</math> for paraffin oil</li> </ul>
China	KN95	GB2626- 2006	NaCl	$0.075 \pm 0.020 \mu\text{m}$ CMD (count median diameter) (GSD < 1.86)
Korea	KF94	KMOEL - 2017-64	NaCl and paraffin oil	<ul style="list-style-type: none"> <li>• 0.02 <math>\mu\text{m}</math> to 2 <math>\mu\text{m}</math> with the average particle size of 0.6 <math>\mu\text{m}</math> for NaCl</li> <li>• 0.05 <math>\mu\text{m}</math> to 1.7 <math>\mu\text{m}</math> with the average particle size of 0.4 <math>\mu\text{m}</math> for paraffin oil</li> </ul>
Non- Regulated	N/A	Viral Filtration Efficiency (referred Nelson Laboratories procedure as an example here)	PhiX174 virus	$3.0 \pm 0.3 \mu\text{m}$ MPS

Table 2- 2 continued:

<b>Country</b>	<b>Mask Type</b>	<b>Flow Rate/Face Velocity</b>	<b>Acceptable FE</b>	<b>Acceptable <math>\Delta P</math></b>
The US	N95 P95	85 L/min of flow rate*	$\geq 95\%$	$\leq 245$ Pa (upon exhalation)
	Surgical Masks	0.5 to 25 cm/s of face velocity 85 L/min of flow rate*	$\geq 95\%$ for Level 1	$< 49$ Pa
Europe	FFP2	95 L/min of flow rate*	$\geq 94\%$	$\leq 240$ Pa at 95 L/min
China	KN95	85 L/min of flow rate*	$\geq 95\%$	$\leq 250$ Pa (upon exhalation)
Korea	KF94	95 L/min of flow rate*	$\geq 94\%$	$\leq 240$ Pa at 95 L/min
Non-Regulated	N/A	28.3 L/min of flow rate*	N/A	N/A

Note:  
\* Face velocity varies between respirators.

### 1.6.1. Working Principles of an Electrical Low Pressure Impactor

In order to measure size-specific FE and to count particles in a wider range of particle sizes, the following chapters incorporated an Electrical Low Pressure Impactor (ELPI) in experiments. To measure FE and pressure drop of masks, TSI Automated Filter Testers are widely used (Bergman et al., 2010; Viscusi et al., 2007), however, the tester provides a single FE averaged over a range of challenge particle sizes and may inaccurately measure the count of ultrafine particles (<100 nm) (Eninger et al., 2008). One of the common setups used in previous literature to measure size-specific FE and to increase the range of measurable particle sizes has been to use more than one particle counter with different operating ranges of particle sizes (Drewnick et al., 2021; Qian et al., 1998; Rengasamy et al., 2010). For instance, Drewnick et al. (2021) used a Condensation Particle Counter for particles between 30 nm and 500 nm and a Scanning Mobility Particle Sizer combined with an Optical Particle Counter for the range between 500 nm and 10  $\mu\text{m}$ . Nonetheless, this method requires multiple measurements for size-specific FE for a single sample and even different types of test aerosols to cover different ranges of sizes. This inconvenience could be alleviated by using an ELPI.

Using particle inertia and charged test particles, ELPI can count particles in different size bins. An ELPI is a cascade impactor that counts the number of different sizes of particles in real-time, including nanoparticles by using low pressure of up to 40 mbar. The low pressure helps achieve higher flow velocities, decreases collection cut points, and collects smaller particles. When particles are forced through jets in each plate, particles smaller than a certain size will remain with the flow and go down to the lower collection plate, while particles larger than a certain size will deviate from the flow and impact the collection plate. Note that, because different particles have different densities, it is common to use aerodynamic diameter which refers to the diameter of a

particle assuming the density of water with the same settling velocity as the actual particle, as shown in Equation 2 - 8 (Finlay, 2019; Hinds, 1999). As particles enter the equipment, it gets charged through corona charging so that when the particle impacts the collection plates, electrometers on the plates can detect the impaction and translate the current from the impaction to counts of particles impacted.

$$d_a = d_p * \left(\frac{\rho_p}{\rho_0}\right)^{1/2} \text{ for spherical particle} \quad \text{Equation 2 - 8}$$

Where  $d_a$  is aerodynamic diameter;  $d_p$  is actual physical diameter;  $\rho_p$  is actual particle density; and  $\rho_0$  is reference particle density (i.e. 1000 kg/m<sup>3</sup>) Note that this equation assumes that 1) particle Re << 1; 2) particle diameter >> mean free path, and 3) gravity and fluid drag are the only external forces on the particle.

For this thesis two different models of ELPI (both, Dekati Ltd., Finland) were used due to different availabilities at the time of experiments: ELPI was first mentioned by Keskinen et al. in 1992, and ELPI+ was introduced in 2010 and has more size bins with finer resolutions (Järvinen et al., 2014). Chapter 3 used ELPI while Chapter 4 utilized ELPI+. See Table 2 - 3 for comparisons of specifications between the two models. Note that in both experiments, full particle size ranges that an ELPI can measure were not used because of the uncertainty in the counts and lack of counts in certain sizes of particles from a nebulizer, which is further explained in each chapter.

Table 2 - 3 Comparison between ELPI and ELPI+

	<b>ELPI (Chapter 3)</b>		<b>ELPI+ (Chapter 4)</b>	
	Full Specification	Range utilized in the experiment	Full Specification	Range utilized in the experiment
<b>Flow Rate</b>	30 L/min		10 L/min	
<b>Number of Stages</b>	12 bins	8 bins	14 bins	10 bins
<b>Range of Aerodynamic Diameter</b>	0.04 µm to 8.15 µm	0.07 µm to 1.97 µm	0.006 µm to 10 µm	0.02 µm to 2.01 µm

### **Chapter 3    Effect of Moist Heat Incubation on Filtration Efficiency of High-Performance Masks**

Decontamination of face masks, such as moist heat incubation is one of the most common treatments done to face masks. This chapter demonstrated the need to use a wider size range of test particles compared to the US National Institute for Occupational Safety and Health (NIOSH)'s test protocol for N-series respirators, and it examined the effect of moist heat incubation which involves high temperature and humidity on respirators' FE and pressure drop.

A similar version of this chapter has been published as: Seo, S., Ruzycki, C. A., Johnson, B., Wang, H., Vehring, R., Romanyk, D., Finlay, W. H., & Martin, A. R. (2022). Size-Specific Filtration Performance of N95 Respirators after Decontamination by Moist Heat Incubation. *Journal of Aerosol Medicine and Pulmonary Drug Delivery*, 35(1), 41–49.

#### 1.7. Introduction

Disposable respirators or filtering facepiece respirators (hereafter referred to as respirators) protect against inhalation exposure to particulate contaminants by maintaining a tighter seal to users' faces, compared to surgical masks, and providing effective filtration over a wide range of particle sizes (Oberg & Brosseau, 2008; WHO, 2020). In North America, certified N95-type respirators with a minimum filtration efficiency (FE) of 95% are widely used for the protection of healthcare workers. These respirators' FEs are tested to be certified by NIOSH as per procedures listed in Title 42 CFR Part 84 (The US Public Health Service, 2012). Similarly, the GB 2626-2006 standard is used to certify KN95 respirators in China and the EN 149-2001 standard is used for FFP2 respirators in Europe (OSHA, 2020). The NIOSH test parameters specified in Title 42 CFR Part 84 Subpart K are intended to provide a challenging scenario for the filtration of small particles and to measure the “worst-case scenario” performance for N-type respirators. These parameters

include a high flow rate of  $85 \pm 4$  L/min, corresponding to a face velocity of 9.3 cm/s for a typical N95 respirator (Rengasamy et al., 2017) (flow rate divided by the cross-sectional area of respirator exposed to the flow); use of sodium chloride (NaCl) test particles with a count median diameter of  $0.075 \pm 0.20$   $\mu\text{m}$  and a standard geometric deviation not exceeding 1.86, based on reported most penetrating particle sizes (0.030  $\mu\text{m}$  to 0.100  $\mu\text{m}$ ) for N-type respirators (He et al., 2013); and test particles that are charge-neutralized to achieve Boltzmann equilibrium, giving lower FE compared to charged particles (Kilic et al., 2017). Before the FE tests, respirators are also preconditioned at 38°C and 85% relative humidity (RH) for 25 hours which may reduce electrostatic deposition (Eninger et al., 2008; Moyer, Ernest S.; Stevens, 1989). The test continues until minimum efficiency is achieved or until a mass of at least  $200 \pm 5$  mg of test particles has contacted the filter.

During pandemics caused by infectious viruses such as SARS-CoV-2 (WHO, 2020) and H1N1 (Bergman et al., 2011) that can transmit through aerosols, demand for respirators has been high. This has led to a shortage of respirators, prompting attempts to increase the supply by decontaminating and reusing available respirators (Ou et al., 2020). There is no official decontamination method for respirators but sterilization by vaporous hydrogen peroxide, ultraviolet germicidal irradiation, and moist heat incubation (MHI) are three decontamination methods recommended by the US Centers for Disease Control and Prevention (CDC, 2020) because they have been shown to disinfect respirators with less impact on their filtering performance and fitting than other methods, such as autoclaving and isopropyl alcohol soaking (Viscusi et al., 2007). For certain techniques such as hydrogen peroxide gas plasma (Bergman et al., 2010; Steinberg et al., 2020), multiple cycles of decontamination can lead to decreased protection for users from the loss of FE or deformation of the respirator seal. For N95-type respirators that often utilize electrostatic (electret) media (Viscusi et al., 2007), electrostatic effects

may decrease from decontamination methods that require high relative humidity and temperatures or chemical disruption of the fiber and consequently decrease FE, especially at larger particle sizes up to 0.4  $\mu\text{m}$  (Martin & Moyer, 2000). To support and ensure the safety of decontaminated respirators, NIOSH's FE tests have been used to quantify the FE of decontaminated NIOSH- and non-NIOSH-certified respirators (Bergman et al., 2011; Daeschler et al., 2020; NPPTL, 2020b). However, the limited range of test particle diameters within the NIOSH test procedure may neglect decreased FE at larger particle diameters and therefore overestimate respirator performance.

We hypothesized that the NIOSH test particle size range may not be sufficient to capture worst-case FE for decontaminated N95 respirators, particularly if a decontamination technique negatively influences the electrostatic properties of the respirator material. Moist heat incubation (MHI) was chosen as the decontamination method in the present study, as it has previously been shown effective in deactivating viruses and bacteria while maintaining respirator integrity (Table 3 - 1). Heimbuch *et al.* found that MHI fully deactivated H1N1 viruses more consistently than ultraviolet germicidal irradiation (Heimbuch et al., 2011). However, previous studies used the limited range of test aerosol sizes defined by NIOSH, or similar, and did not measure particle-size-specific FE. Therefore, we utilized a custom experimental apparatus to extend the range of test particle sizes and to measure FE at different test particle size bins. The FE, pressure drop, and physical integrity of two different, commercially available N95 respirator models labeled as providing at least 95% FE were investigated before and after ten cycles of MHI decontamination.



Table 3 - 1 Comparisons between current and previous studies on the effects of moist heat incubation (MHI) on respirators

	Current Study	(Heimbuch et al., 2011)	(Bergman et al., 2011)	(Daeschler et al., 2020)		
Respirator Tested	<ul style="list-style-type: none"> <li>Kimtech™ N95 53358</li> <li>Medstar KN95</li> <li>Safe Life N95 B130</li> </ul>	<ul style="list-style-type: none"> <li>Three NIOSH- and FDA-approved N95 surgical respirators</li> <li>Three NIOSH-approved N95 particulate respirators</li> </ul> <p>(Makes and brand names anonymized)</p>	<ul style="list-style-type: none"> <li>3M 1860</li> <li>3M 1870</li> <li>Kimberly Clark PFR95-270 (46767)</li> </ul>	<ul style="list-style-type: none"> <li>3M 1860</li> <li>3M 8110</li> <li>3M 8210</li> <li>3M 9105</li> </ul>		
Number of Decontamination Cycles	10	1	3	10		
Heating Condition	59 ± 1°C and 67 ± 2% RH for 30 minutes	65°C ± 5°C and 85 ± 5% RH for 30 minutes	60°C and 80% RH for 15 minutes	70°C and 50% RH for 60 minutes	70°C and 0% RH for 60 minutes*	
Drying/Cooling Condition	59 ± 1°C and 11 ± 2% RH for 30 minutes	Not described	Not described	Room temperature for 5 minutes mid-cycle	Room temperature for 5 minutes mid-cycle	
Range of NaCl Test Particle Used	Wider than NIOSH's range: aerodynamic diameter 0.07 to 1.97 µm (approx. count diameter 0.05 to 1.34 µm)	Not tested against test particles	Same as NIOSH's range: count median diameter of 0.075 ± 0.020 µm and a geometric standard deviation of less than 1.86	Similar to NIOSH's range: count median diameter of 0.075 ± 0.020 µm		

Table 3 - 1 continued:

	<b>Current Study</b>	<b>(Heimbuch et al., 2011)</b>	<b>(Bergman et al., 2011)</b>	<b>(Daeschler et al., 2020)</b>
Physical Degradation	See Results	No obvious visual deterioration	Mean face seal leakage <1% throughout the three cycles of decontamination	Minimal change in fiber diameter No drop in filtration efficiency
Microbial Inactivation	Not examined	> 4 log reduction of H1N1	Not examined	Density of <i>E. coli</i> decreased from 2.77 to 0.02 through optical density measurement No infectious SARS-CoV-2 detected

\*Note that this dry heat condition (0% RH) is not an example of moist heat decontamination, however, it demonstrated that SARS-CoV-2 are susceptible to destruction under high temperature. This implies that it will be more susceptible to destruction under high temperature accompanied by high humidity as moist heat can destroy proteins more efficiently than dry heat (Fairbrother, 1945).

## 1.8. Method

### 1.8.1. Respirator Selection

Two respirator models including the Kimtech™ N95 (53358; Kimberly-Clark Corp., Roswell, GA, USA) and the Safe Life N95 (B130; Safe Life Corp., San Diego, CA, USA) were selected for testing. Two different models were deemed a sufficiently large enough sample group, as the aim of this study was to assess a respirator test methodology evaluating size-specific FE, and not to broadly assess the performance of certified versus non-certified respirators. The Kimtech™ N95 53358 is a NIOSH-certified N95 particulate filter respirator (approval number TC-84A-9042) and was acquired through Fisher Scientific in 2020. The Kimtech™ respirators did not have an expiry date indicated but were considered not expired as they were stored for a maximum of 5 months since their manufacturing date prior to the test: most N95 respirators are likely to maintain the required FE after 10 years. (Viscusi et al., 2009) The Safe Life N95 B130 has not been NIOSH-certified since 2015 but it was used in this study as its stockpile was considered for use during the COVID-19 pandemic. (NPPTL, 2020a) The Safe Life respirators were donated from a stockpile of respirators at the University of North Carolina, with a limited sample shipped to Edmonton for inclusion in the present study. The Safe Life respirators did not have the expiry date indicated and were considered near expiration as they were stored for approximately 10 years since their addition to the University of North Carolina's stockpile. For each respirator model, three respirators were randomly selected for the control group and another three for the decontaminated group.

### 1.8.2. Moist Heat Incubation Decontamination

Respirators were decontaminated in an environmental chamber (Lunaire CEO910W-4; Thermal Product Solutions, Williamsport, PA, USA) with temperature and humidity control. In

each round of decontamination, the decontaminated respirators were conditioned at an average temperature of  $59 \pm 1^\circ\text{C}$  and  $67 \pm 2\%$  relative humidity (RH) for 30 minutes, then dried at  $59 \pm 1^\circ\text{C}$  and  $11 \pm 2\%$  RH for another 30 minutes. This was repeated ten times for each sample in the decontaminated group. All respirators were transferred in sealed Ziploc bags at room temperature and tested for FE within 4 days after decontamination.

### 1.8.3. Filtration Efficiency Test

Before each FE test, both control and decontaminated respirator samples were preconditioned at  $38^\circ\text{C}$  and 85% RH for 25 hours in the environmental chamber and tested within ten hours, consistent with test procedures outlined in Title 42 CFR Part 84 Subpart K. Previously developed methods (Mao et al., 2008; Tavernini et al., 2018) were modified to measure FE and pressure drop across respirators using the experimental setup detailed in Figure 3 - 1. Isotonic saline (0.9% w/v of NaCl) was nebulized with a 6-jet nebulizer (Collison Nebulizer; CH Technologies, Westwood, NJ, USA) using compressed dry air at a pressure of 138 kPa (20 psi). Emitted droplets were neutralized to a Boltzmann distribution using a Kr-85 charge neutralizer and then dried to solid particles through a silica gel drying column. The test particles, after being well-mixed at the top of a large plenum through two fans, settled into the main chamber of the plenum through a hexagonal mesh serving as a flow straightener. Sample holders on the blank and filter lines were designed such that a 5.72 cm by 8.26 cm (2.25 in by 3.25 in) cutout of respirator material was exposed to the constant 30 L/min flowrate generated by the vacuum pump (the flow rate specification of the electrical low pressure impactor noted below), which corresponds to a face velocity of 10.6 cm/s – similar to the typical NIOSH respirator testing at 9.3 cm/s. Face velocity, rather than flow rate, is the more important factor in determining FE according to single-fiber filtration theory (Hinds, 1999), and other studies also have used different flow rates to achieve face

velocities similar to NIOSH’s or real-life situations (Hao et al., 2020; Li et al., 2012). Hence, measurements obtained using the present setup were expected to be comparable to those achieved in a standard respirator test per Title 42 CFR Part 84 for N95 respirators.

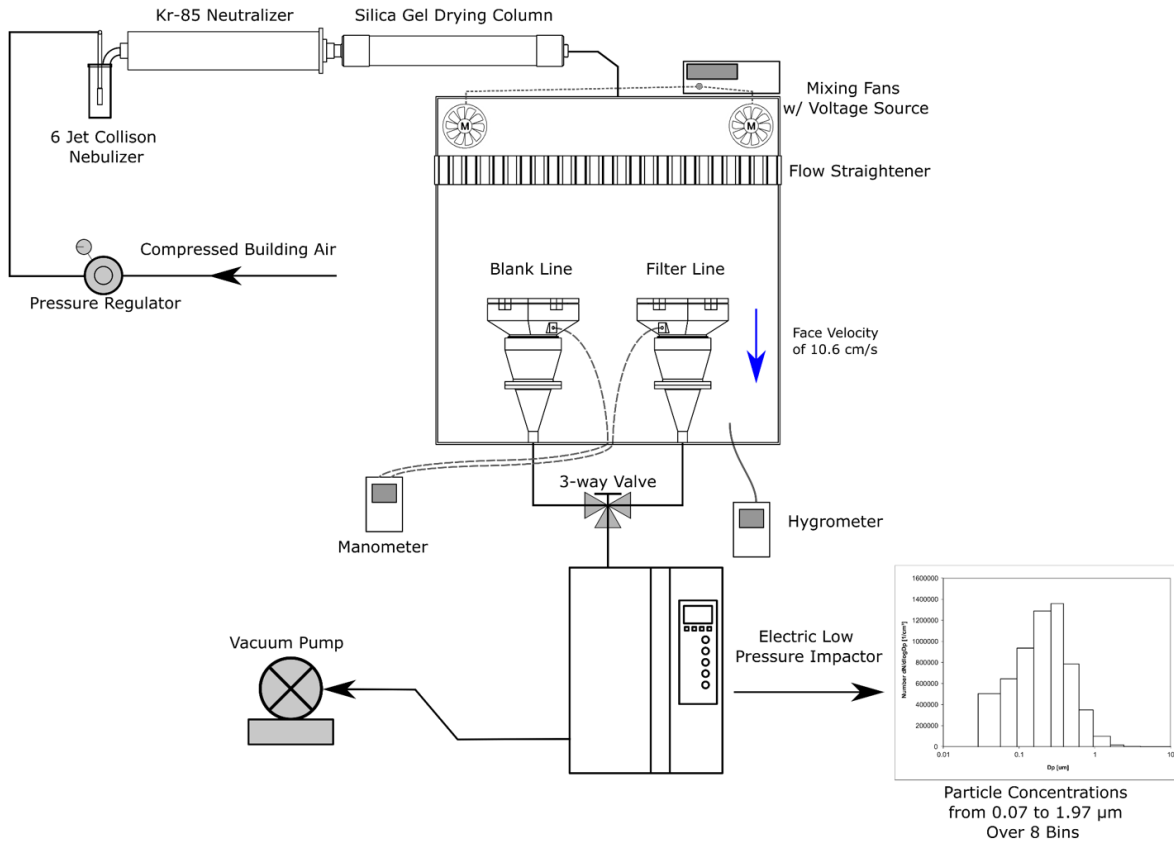


*Figure 3 - 1 Experimental setup used to quantify filtration efficiencies across a range of particle sizes and pressure drops. A comparison of number concentrations measured by Electric Low Pressure Impactor in the blank and filter lines drawing from well-mixed test particles in a large plenum allowed quantification of filtration efficiencies across various particle sizes.*

Particle concentrations,  $C$ , in each line were measured with an electrical low pressure impactor (ELPI; Dekati Ltd., Kangasala, Finland). Note that, in this chapter, an older version of ELPI was used. See Chapter 2 for details on the comparison between ELPI and ELPI+. Concentrations were averaged over three 100-second periods in the blank line ( $C_{\text{challenge}}$ ) and averaged over two 100-second periods in the filter line ( $C_{\text{filtered}}$ ). The ELPI continuously measured particle concentration as a function of aerodynamic particle size in 12 discrete bins

bounded by aerodynamic diameters ranging from 0.04  $\mu\text{m}$  to 8.15  $\mu\text{m}$ . For this study, only size bins in the range from 0.07  $\mu\text{m}$  to 1.97  $\mu\text{m}$  were used, because particle concentrations outside of this range required over 15% correction on raw measurements to compensate for charger efficiency, bouncing, diffusion, and space charge, and because concentration for particles larger than 1.97  $\mu\text{m}$  was less than 0.1% of total concentration. The chosen range was deemed sufficient as it included NIOSH's standard test particle range (for which 68% of particles have aerodynamic diameters between 0.06  $\mu\text{m}$  to 0.21  $\mu\text{m}$  – as calculated from the nominal count median diameter and geometric standard deviation specified in Title 42 CFR Part 84), but expanded the range to larger particle sizes. The FE in each  $i$ -th bin,  $FE_i$ , was then determined using Equation 3 - 1.

$$FE_i = 1 - \frac{C_{\text{filter},i}}{C_{\text{challenge},i}} \quad \text{Equation 3 - 1}$$

A manometer was connected between the blank and filter lines to measure pressure drop downstream of the respirator material. Three replicates were performed for each group. Environmental conditions within the plenum during testing were as follows: ambient pressure of  $93 \pm 1$  kPa; temperature of  $23 \pm 1^\circ\text{C}$ ; and relative humidity of  $34 \pm 7\%$  RH.

#### 1.8.4. SEM Image

Field emission scanning electron microscopy (Zeiss Sigma FE-SEM; Carl Zeiss, Oberkochen, Germany) was used to investigate any possible physical deteriorations in respirator filter layers after decontamination. FE-SEM was operated at electron high tension of 4.00 kV and imaged the filter layers at the magnifications of x40 and x100. The filter layers mounted onto carbon tape were placed over aluminum stubs. Prepared stubs were subsequently coated with gold (Denton Vacuum Desk II Sputter Coater; Denton, Moorestown, NJ, USA) to a thickness of approximately 16 nm.

### 1.8.5. Statistical Analysis

Means are expressed with standard deviation over repeated tests as mean±SD. Statistical analysis was performed on FE and pressure drop data. For FE, decontaminated respirators were compared with the control group using a two-way analysis of variance (ANOVA). For pressure drop, the decontaminated group was compared with the control using a two-sample t-test assuming unequal variances. Both analyses assumed a 95% confidence level.

### 1.9. Results

The size-specific FEs of the two different respirator models before and after ten cycles of MHI are shown in Figure 3 - 2, in which the standard NIOSH test particle size range (aerodynamic diameters between 0.06  $\mu\text{m}$  to 0.21  $\mu\text{m}$ ) is indicated as a grey area. The most penetrating particle sizes (MPPS) and corresponding FE are tabulated in Table 3 - 2. NIOSH-certified Kimtech<sup>TM</sup> N95 respirators maintained a FE greater than 98% across the size range of test particles both before and after decontamination cycles. The change in FE between the control and MHI groups was 0.4% on average which was not significant ( $p > 0.05$ ). The FE of the non-NIOSH-certified Safe Life N95 respirator dropped on average by 6.3% after decontamination, which was statistically significant ( $p < 0.05$ ). The MPPS of Safe Life respirators were found to be outside the NIOSH test particle range in both control and decontaminated groups, and the largest drop of 8.4% in FE occurred at 0.49  $\mu\text{m}$ . It was also found that after ten cycles of MHI, Safe Life respirators' MPPS shifted to a larger particle size, from 0.32  $\mu\text{m}$  to 0.49  $\mu\text{m}$ .

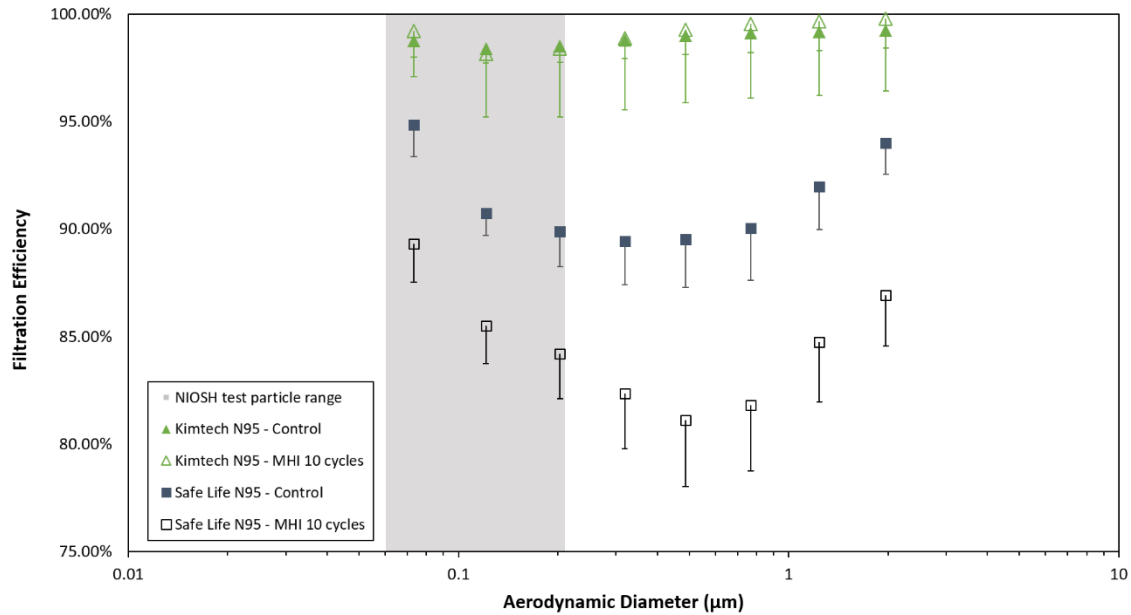


Figure 3 - 2 Filtration efficiencies from commercial N95s before and after ten cycles of moist heat incubation (MHI). Grey area indicates typical NIOSH test particle sizes (aerodynamic diameter of 0.06  $\mu\text{m}$  to 0.21  $\mu\text{m}$ ). For clarity, only negative error bars are depicted.

Table 3 - 2 Filtration efficiency (FE) at the most penetrating particle size (MPPS) before and after ten cycles of moist heat incubation (MHI)

		Kimtech™ N95	Safe Life N95
<b>Control</b>	FE	98.4 ± 0.7%	89.4 ± 2.0%
	MPPS	0.12 $\mu\text{m}$	0.32 $\mu\text{m}$
<b>After Ten Cycles of MHI</b>	FE	98.2 ± 0.0%	81.1 ± 3.1%
	MPPS	0.12 $\mu\text{m}$	0.49 $\mu\text{m}$

Ten cycles of MHI did not have an appreciable influence on the pressure drop through respirator samples (Table 3 - 3). For the Kimtech™ respirator, differences in pressure drop before and after MHI were not statistically significant ( $p > 0.05$ ). For the Safe Life respirator, pressure drop decreased after decontamination ( $p = 0.04$ ), but the decrease of 12 Pa was deemed negligible from a practical perspective. As shown in SEM images (Figure 3 - 3), there were no obvious visible changes to filter layers for any of the respirators.

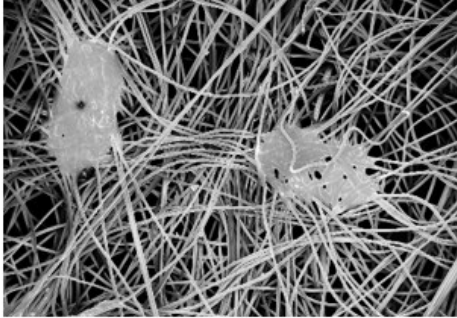
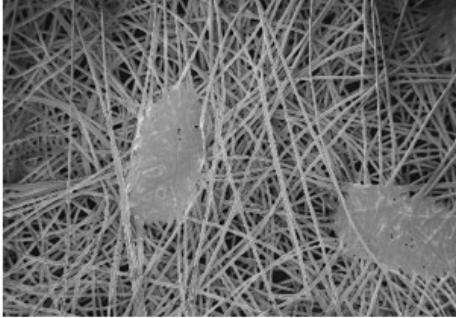
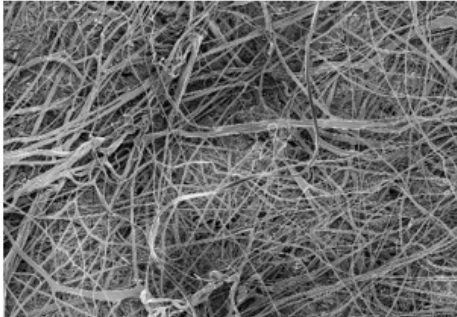
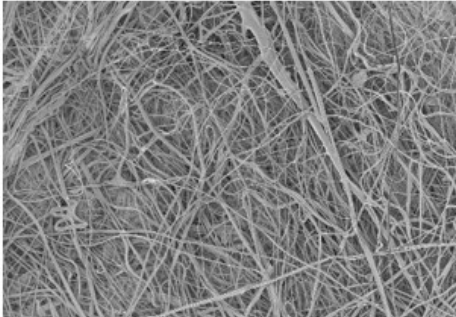
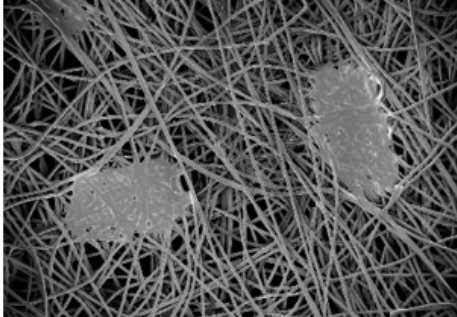
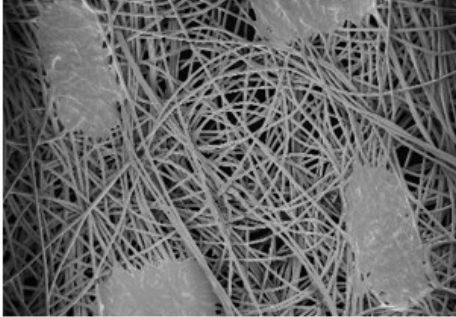


*Table 3 - 3 Pressure drops across commercial N95s before and after ten cycles of moist heat incubation (MHI)*

	<b>Kimtech™ N95</b>	<b>Safe Life N95</b>
<b>Control</b>	106 ± 4 Pa	64 ± 4 Pa
<b>After Ten Cycles of MHI</b>	109 ± 1 Pa	52 ± 1 Pa

#### 1.10. Discussion

In the present study, multiple cycles of moist heat incubation did not compromise the FE of the NIOSH-certified N95 respirator tested, the Kimtech™ N95, which agrees with findings in previous studies for different models of certified N95 respirators (Bergman et al., 2010, 2011; Viscusi et al., 2011). However, this result was not consistent across the two high-efficiency respirator models tested. For the non-NIOSH-certified Safe Life respirators, FE was reduced across all tested particle sizes after ten cycles of MHI. Furthermore, the most penetrating particle sizes shifted to larger particle sizes, outside the range of those tested in the NIOSH test standard (aerodynamic diameter 0.06 µm to 0.21 µm). It was initially assumed that the decreased FE would have been mainly caused by either physical deterioration in fibers or decreased electrostatic effect. As SEM images showed that the respirators' fibers were not physically degraded, this decrease in FE and the shift in the most penetrating particle sizes to 0.49 µm may be due to deterioration in electrostatic filtration after exposure to high temperature and humidity. For N95-type respirators in which electrostatic effects play a major role in enhancing FE, the most penetrating particle size tends to lie below 0.10 µm (Li et al., 2012). In contrast, materials that do not have a strong electrostatic effect exhibit most penetrating particle sizes above 0.25 µm, as shown in previous studies in which electrostatic forces have been removed, e.g. by exposure to isopropanol (Martin & Moyer, 2000).

	Kimtech™ N95	
	Control	After Ten Cycles of MHI
<b>Outer-most Layer</b> (Mag 40x) 500 μm ↔		
<b>Middle Layer</b> (Mag 100x) 100 μm ↔		
<b>Inner-most Layer</b> (Mag 40x) 500 μm ↔		

*Figure 3 - 3 SEM images of commercial N95 respirators before and after ten cycles of moist heat incubation (MHI).*

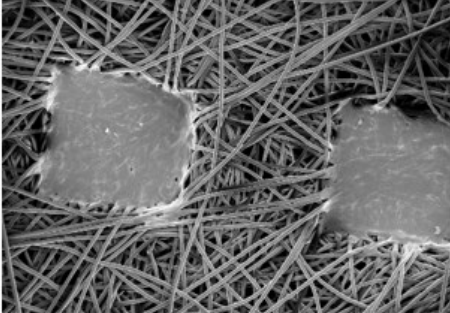
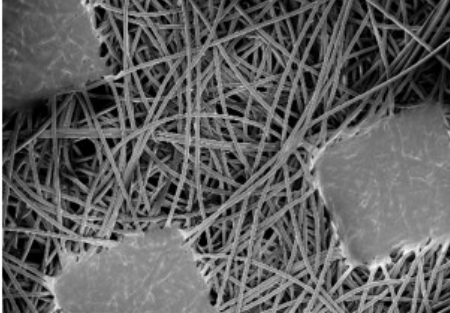
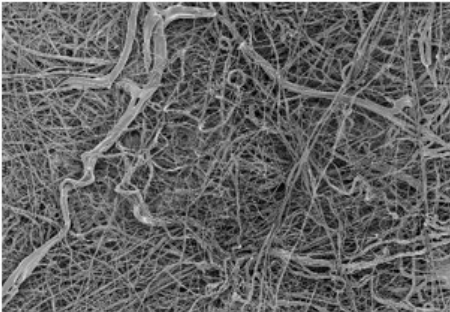
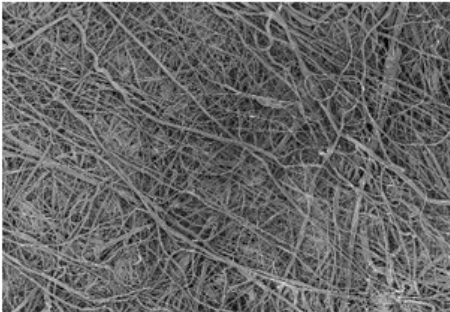
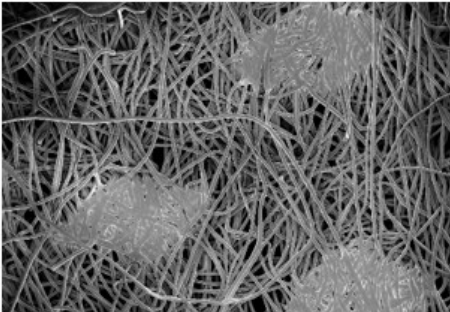
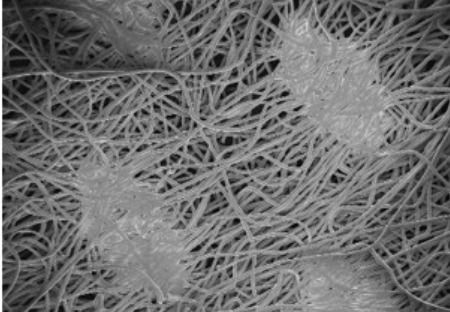
	Safe Life N95	
	Control	After Ten Cycles of MHI
<b>Outer-most Layer</b> (Mag 40x) 500 $\mu$ m $\longleftrightarrow$		
<b>Middle Layer</b> (Mag 100x) 100 $\mu$ m $\leftrightarrow$		
<b>Inner-most Layer</b> (Mag 40x) 500 $\mu$ m $\longleftrightarrow$		

Figure 3 - 3 (continued) SEM images of commercial N95 respirators before and after ten cycles of moist heat incubation (MHI).

It is important to note that respirator certification tests defined by NIOSH and other agencies have been developed to assess protection against a broad range of hazardous aerosols, including dust, fumes, and mists that may be encountered in a workplace setting. Many of these aerosols contain smaller particles than the sizes encountered in the context of protection against infectious aerosols. For instance, the diameter of the SARS-CoV-2 virus is approximately 0.06  $\mu\text{m}$  to 0.14  $\mu\text{m}$ (Bar-On et al., 2020) and infectious aerosol particles containing virus must be at least as large as the virus itself, owing to components of lung fluid, saliva, or mucus which will remain even after rapid evaporation of water from exhaled droplets(Marr et al., 2019). As a result, the relevant size range for infectious aerosols may exceed the size range used in NIOSH certification testing, and filtration at such sizes cannot be readily inferred from the results of certification testing. The risk associated with neglecting to test filtration for larger particles is greater for infectious aerosols than for many workplace aerosols because larger particles are capable of containing higher viral loads owing to their increased volume. These considerations suggest that for assessing protection against infectious aerosols, respirator FE should be measured at diameters larger than specified in NIOSH test protocol, especially after decontamination cycles that can reduce electrostatic filtration, and for non-certified respirators or homemade masks (Rengasamy et al., 2010) that may underperform at larger particles sizes. Reporting FE only within the NIOSH test particle range, or at a specific particle size(Fisher et al., 2011; L. Liao et al., 2020; Lore et al., 2012), may not adequately characterize respirator performance against infectious aerosols, and not capture actual worst-case scenarios.

A limitation of the present study is the limited number of samples and the limited pool of respirator types and models tested, as well as the lack of full details of the previous storage conditions, especially for the Safe Life respirators. It is uncertain whether the FE measured for

control Safe Life respirators without MHI is reflective of the respirator design itself (Viscusi et al., 2009), the specific samples tested, or whether FE was influenced by storage conditions, for example, high humidity (Mahdavi et al., 2015). Independent NIOSH test results provided through the US National Personal Protective Technology Laboratory's (NPPTL) beyond-shelf-life and stockpiled respirator assessment indicates that FE for Safe Life B130 respirators which are from three different lot numbers and sourced from at least two different storage facilities, varied from 89.8% to 99.7%. (NPPTL, 2020a) In the present study, FE evaluated for control Safe Life B130 respirators within NIOSH test particle sizes is in the range of the NPPTL test results. However, it should be noted that NIOSH does not have requirements for shelf life or storage conditions for particulate-only air-purifying respirators (NPPTL, 2020a) such as N95 hence it is uncertain whether the length of storage and/or storage conditions influenced FE in NPPTL results as well. Due to the lack of records on the past history of respirators, the relationship between long-term storage conditions and degradation of respirators requires further investigation. Regardless, the present study demonstrates the utility of size-specific FE measurement to identify the most penetrating particle sizes, before or after storage, and to evaluate FE at these sizes. Future studies to test size-specific FE of respirators under different MHI temperature or RH conditions and other decontamination methods are also warranted.

Another limitation of the present study was that the same respirator samples were not used before and after MHI. Measuring FE of a new respirator and then using the same respirator to decontaminate and measure FE after MHI may have minimized any variations amongst the samples. However, the incremental addition of NaCl aerosol over multiple tests may result in unintended degradation in FE (Moyer & Bergman, 2000), while this study intended to explore the isolated effect of MHI. Hence, in order to eliminate the possibility that NaCl deposition itself could

influence FE measured after decontamination, we chose to use different respirator samples before and after MHI.

#### 1.11. Conclusion

Two different, commercially available N95 respirator models were decontaminated through ten cycles of MHI, and their FEs were tested in a custom experimental set-up utilizing a range of particle sizes wider than the standard NIOSH respirator certification tests. The encouraging results of the present study for one of the two respirator models studied, coupled with other studies in the literature, suggest that MHI can provide an effective method for decontaminating N95s for reuse. However, for the other respirator model studied, FE was below 95% before MHI cycles and decreased significantly after MHI cycles. Moreover, the most penetrating particle size for this respirator was outside the range defined in NIOSH certification testing and increased after MHI cycles. The ability to evaluate size-specific FE across a wide range of particle sizes, as presented herein, is important in identifying the most penetrating particle size and associated FE of respirators.

## **Chapter 4 Effect of Children's Expected Face Velocity on Filtration Efficiency of Children's Masks**

Using a similar experiment set up which was proven effective to measure minimum FE in Chapter 3, the effect of face velocity on children's masks was examined by comparing FE and pressure drops at two different face velocities, one representative of adults and another of school-aged children.

### 1.12. Introduction

Face masks and respirators have been shown to help protect users against harmful particulate matter including pathogen-containing bioaerosols and pollutants (Howard et al., 2021; Locke et al., 2021; Mueller et al., 2018; Zhou et al., 2018). The FE of face masks, however, has been studied primarily in the context of masks designed for adults, with adult breathing profiles assumed. Little literature on children's mask performance is currently available (Eberhart et al., 2021). When determining mask performance, it is important to distinguish between children and adults because the differences in their respective breathing patterns can influence both the size of the most penetrating particles and the FE offered by the mask materials. The dimensions of children's airways are narrower and shorter than adults (Hofmann, 2011; Xi et al., 2012), and children's breathing patterns are characterized by a higher breathing frequency, smaller tidal volume, lower minute volume, and higher ratio of oral breathing during exercise (Brown et al., 2013; ICRP, 1994). These differences may influence children's vulnerability to a wide range of particle sizes by altering regional airway deposition patterns. (Golshahi et al., 2011) Furthermore, the lower minute volume for children and the smaller surface area of their masks can lead to differences in face velocities through masks (flow rate divided by the material surface area). According to single-fiber filtration theory, face velocity is a key factor affecting filtration through

various mechanisms, including diffusion, inertial impaction, gravitational settling, and electrostatics (Hinds, 1999). Because of these differences, it is crucial to consider child-specific breathing conditions and size-specific FEs when assessing the filtration performance of children's masks.

Despite the differences between children and adults, a standard against which to verify the FE of children's masks has yet to be established. China's standard codes T/CNTAC 55-2020 & T/CNITA 09104-2020 mention children's masks, but emphasize only the respective differences in physical sizes of the masks and airflow resistance for children and adults (M. Liao et al., 2021) without offering a desired FE benchmark or a range of particle sizes that could be easier for children to inhale. In the absence of test standards for any special condition like decontaminated masks or cloth masks, the US National Institute for Occupational Safety & Health's (NIOSH) certification procedure for non-powered particulate masks has often been used or modified to test the FE of masks (Ju et al., 2021). NIOSH's method is generally preferred to other methods like the US Food and Drug Administration's particulate FE tests because the NIOSH test method imposes a worst-case scenario for FE by, for instance, incorporating charge-neutralized sodium chloride particles as test aerosols at a relatively high flow rate (Rengasamy et al., 2017). However, the constant flow rate used during the procedure, 85 L/min, is based on a minute volume for adults under a heavy workload (Janssen et al., 2005), which is typically higher than a child's flow rate under similar conditions (ICRP, 1994). Previous studies have examined the effect of lower flow rates and face velocities on the FE of different mask materials (Drewnick et al., 2021; Guha et al., 2015; Qian et al., 1998; Rengasamy et al., 2020), but the types of masks tested were limited mostly to adult masks. Furthermore, these studies often used fixed flow rates through the whole surface



of the masks, which leads to different face velocities for masks with different surface area and complicates the interpretation of FE relative to different mask materials.

The objective of the present work was to evaluate the FE, pressure drop, and filter quality of masks intended for use by children, including surgical, KN95, cotton, and mixed-material masks, using a face velocity representative of children's high-workload breathing patterns. FE, pressure drop, and filter quality were also assessed with a face velocity representative of adult's high workload breathing rates to inform how typical testing of mask performance using adult parameters may bias results for masks meant for use with children.

### 1.13. Method

#### 1.13.1. Masks Selection

One type of adult N95 respirator, serving as a control, and nine different types of children's masks were tested. The children's masks were selected to represent two different types: nonwoven (KN95 and surgical masks) and woven (100% cotton and mixed-material masks). KN95 and surgical masks were considered nonwoven because the majority of their filtering bodies are composed of nonwoven materials (Forouzandeh et al., 2021), i.e. "a random array of fibers or filaments" including spun-bonded, melt-blown, or electro-spun textiles (Hutten, 2007). Any masks based on cotton combined with other materials such as polyester, spandex, or rayon are hereinafter referred to as "mixed-material."

The target age, dimensions, and composition of each mask are listed in Table 4 - 1. For each mask and face velocity combination, four samples were tested based on a sample size estimate with a minimum expected difference in FE of 10% absolute, a standard deviation of 5% absolute estimated from the previous study in Chapter 3 with similar setup (Seo et al., 2022), desired power of 0.8, and two-tailed significance criterion of 0.05. All samples were preconditioned at  $85 \pm 5$  %

relative humidity and  $38 \pm 2.5$  °C for  $25 \pm 1$  hours before testing, as per requirements for non-powered air-purifying particulate respirators listed in Title 42 CFR Part 84 (The US Public Health Service, 2012).

#### 1.13.2. Basis of the Face Velocities

Two different constant flow rates were chosen to represent the minute volumes of adults and children under high workloads. The minute volume can be calculated by dividing the sum of all instantaneous inspiratory airflows by time duration (Janssen et al., 2005). The flow rate of 85 L/min was assumed for adults' typical minute volume as per 42 CFR 84 Subpart K and as per Janssen et al.'s 50<sup>th</sup> percentile minute volume for men over 20 years old at the high work rate (80% of each subject's  $VO_{2,max}$ ) (Janssen et al., 2005). For school-aged children (6 to 11 years old), minute volumes of 33.7 L/min were estimated in accordance with the sources listed in Table 4 - 2. Because face velocity is a critical factor in determining FE according to single-fiber filtration theory (Hinds, 1999), face velocities were then calculated using assumed mask areas exposed to flow. With a typical respirator surface area of 150 cm<sup>2</sup> (Rengasamy et al., 2017), a face velocity of 9.3 cm/s was assumed for adults. For children's masks, the estimate was based on the advertised dimensions given by manufacturers with the average surface area of 141 cm<sup>2</sup> yielding a face velocity of 4.0 cm/s for school-aged children.

Table 4 - 1 Masks specifications

Type	Mask	Model	Target Age [year]	Approximate Surface Area Based on Advertisement [m <sup>2</sup> ]	Note
Control	AdultN95	Kimtech™ 53358	N/A	0.014	NIOSH-Approved (TC# 84A-9042)
	Children KN95	VIDA KN95	+10	0.0215	FDA Registered #3017171515
Nonwoven	Children Surgical1	Trana Surgical Face Mask ASTM Level3	3 to 12	0.0138	Health Canada issued Medical Device Establishment License #13866
	Children Surgical2	Thinka Children Surgical Mask ASTM Level1	2 to 8	0.0126	Health Canada Medical Device Establishment License. License Number: 12163
	Children Surgical3	Dent X 3 Ply Kids, ASTM Level3	6 to 16	0.0125	N/A
Woven	Children Cotton1	Old Navy Non-medical-grade Face Masks	+3	0.0116	N/A
	Children Cotton2	GAP Accordion Non-medical-grade Face Mask	+4	0.0106	N/A
	Children Mix1	Hanes Kids' Face Mask	5 to 12	N/A	N/A
	Children Mix2	GAP Minion Face Coverings	+4	0.0106	N/A
	Children Mix3	Weddingstar 3-ply Kid's Washable Cloth Face Mask	+3	0.0194	N/A

Table 4 - 1 continued:

Type	Mask	Model	Composition
Control	AdultN95	Kimtech™ 53358	3 Layers Nonwoven
Nonwoven	Children KN95	VIDA KN95	3 layer 30% Non-Woven Polypropylene Fabric, 20% Meltblown Polypropylene Fabric, 50% ES Hot Air Cotton
	Children Surgical1	Trana Surgical Face Mask ASTM Level3	Three layers. Non-woven and melt-blown fabrics
	Children Surgical2	Thinka Children Surgical Mask ASTM Level1	Three layers. Two non-woven, middle melt-blown.
	Children Surgical3	Dent X 3 Ply Kids, ASTM Level3	3 Layer Polypropylene non-woven
	Children Cotton1	Old Navy Non-medical-grade Face Masks	3 Layer 100% cotton
Woven	Children Cotton2	GAP Accordion Non-medical-grade Face Mask	Three layer 100% cotton
	Children Mix1	Hanes Kids' Face Mask	2 Layer 60% cotton and 40% polyester
	Children Mix2	GAP Minion Face Coverings	Two-layer Shell: 96% polyester and 4% spandex Lining: 96% cotton and 4% spandex
	Children Mix3	Weddingstar 3-ply Kid's Washable Cloth Face Mask	Three-layer Two layers of 100% cotton One layer of 100% rayon

Table 4 - 2 Children's inhalation rates during high workload from previous literature

Source	Age [year]	Gender	Activity Level	Minute Volume Rate [L/min]
International Commission on Radiological Protection (ICRP) 1994 Table B.15 (ICRP, 1994)	5	Male	Heavy exercise (64% workload)	37
	10	Female	Heavy exercise (64% workload)	31
Roy and Courtay Table 3 (Roy, Monique. Courtay, 1991)	6	N/A	Heavy exercise (64% workload)	18.5
	12	Male	Heavy exercise (64% workload)	40.3
The US Environmental Protection Agency (EPA) 2009 Table C-4 (U.S. Environmental Protection Agency (EPA), 2009)	6 to 11	Male 50 <sup>th</sup> percentile	High intensity (Metabolic equivalent > 6.0)	41.9
<b>Average Flow Rate</b>				<b>33.7</b>

### 1.13.3. Experiment Setup

A custom-designed setup with an Electrical Low Pressure Impactor (ELPI+; Dekati Ltd., Finland) similar to the one described in Seo et al. (Seo et al., 2022) was used to measure FE at the two different face velocities. A diagram of the experimental apparatus is shown in Figure 4 - 1. Note that, in this chapter, a newer version of ELPI was used. See Chapter 2 for details on the comparison between ELPI and ELPI+. Nebulized isotonic saline (0.9% w/v NaCl) droplets were neutralized and dried before entering a plenum. Resultant particles were pulled by a vacuum pump in line (A) in Figure 4 - 1 and, using a 3-way valve and were passed through either a blank or filter line with a cut-out cross-section area sized 5.72 cm by 8.26 cm (2.25 in by 3.25 in). The cut-outs of masks were secured in an airtight manner in the filter line. To ensure that smaller particles were collected with minimal bouncing, greased sintered plates were used in the ELPI+. One of the problems with the ELPI in Chapter 3 was uncertainty in the counts of smaller particles due to particles bouncing off the aluminum foil on collection plates. To mitigate the issue, sintered metal

plates were used in this chapter. The sintered metal plates have oil that seeps up through pores to continuously bundle incoming particles and helps collect 10 to 20 times more particles than the normal collection plate. (Dekati Ltd, 2018)

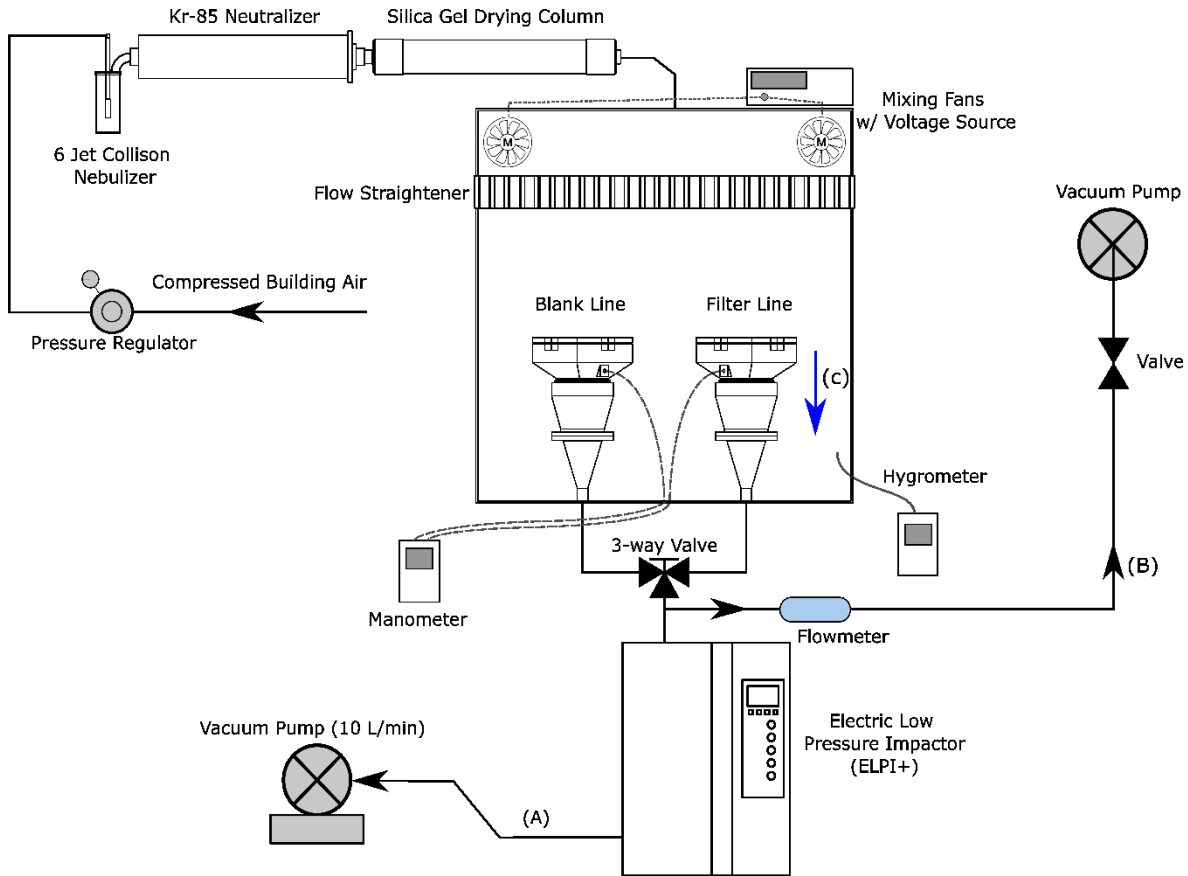


Figure 4 - 1 Experiment set-up to measure pressure drop and size-specific material filtration efficiency

The nominal airflow was set to 10 L/min as specified by the ELPI+ in line (A) in Figure 4 - 1. A second pump through line (B) in Figure 4 - 1 provided additional flow rate to yield a lower flow rate at the cut-out or suction to yield a higher flow rate so that different face velocities of  $9.37 \pm 0.12$  cm/s and  $4.01 \pm 0.00$  cm/s could be applied at the filters (point (C) in Figure 4 - 1) by creating respective resultant flow rates of 16.5 L/min and 1.36 L/min. The ELPI+ continuously measured particle concentration as a function of aerodynamic particle size in 10 discrete bins

ranging between 0.02 and 2.01  $\mu\text{m}$  (the geometric mean diameters of two neighboring channels). While the ELPI+ is capable of measuring particles with an aerodynamic diameter ranging from 0.01 to 7.24  $\mu\text{m}$ , the nebulizer used in the present study produced particles only in the size bins from 0.02 to 2.01  $\mu\text{m}$ . This was deemed an acceptable range as it encompasses the standard NIOSH test particle size range, for which 68% of particles have aerodynamic diameters between 0.06  $\mu\text{m}$  to 0.21  $\mu\text{m}$ . Particle concentrations were averaged over three 90-second periods in the blank line ( $C_{\text{challenge}}$ ) and over two 90-second periods in the filter line ( $C_{\text{filtered}}$ ). Note that the length of each period is 10 seconds less compared to Chapter 3 as the ELPI+ reached the maximum collection limit faster than ELPI so the duration was shortened. FE in each,  $i$ -th, particle size bin was then calculated using Equation 4 - 1.

$$FE_i = 1 - \frac{C_{\text{filtered},i}}{C_{\text{challenge},i}} \quad \text{Equation 4 - 1}$$

The NaCl size distribution of the challenge aerosol used in this experiment had a geometric mean aerodynamic diameter of 0.05  $\mu\text{m}$  with a geometric standard deviation of 2.6, based on the blank line concentrations measured by the ELPI+. A manometer was connected between the blank and filter lines to measure pressure drop downstream of the respirator material. Environmental conditions within the plenum during testing were as follows: ambient pressure of  $93 \pm 1$  kPa; temperature of  $21 \pm 2$  °C; and relative humidity of  $31 \pm 6$  %RH.

One of the primary concerns for children is breathability (Villani et al., 2020). Hence, to evaluate any changes in FE compared to the change in pressure drop experienced by the user, the filter quality ( $q_F$ ) (Hinds, 1999) was calculated using Equation 4 - 2.

$$q_F = \frac{\ln\left(\frac{1}{1 - FE_{\text{min}}}\right)}{\Delta P} \quad \text{Equation 4 - 2}$$

Here  $\Delta P$  is the pressure drop in Pa and  $FE_{\text{min}}$  is the minimum FE.

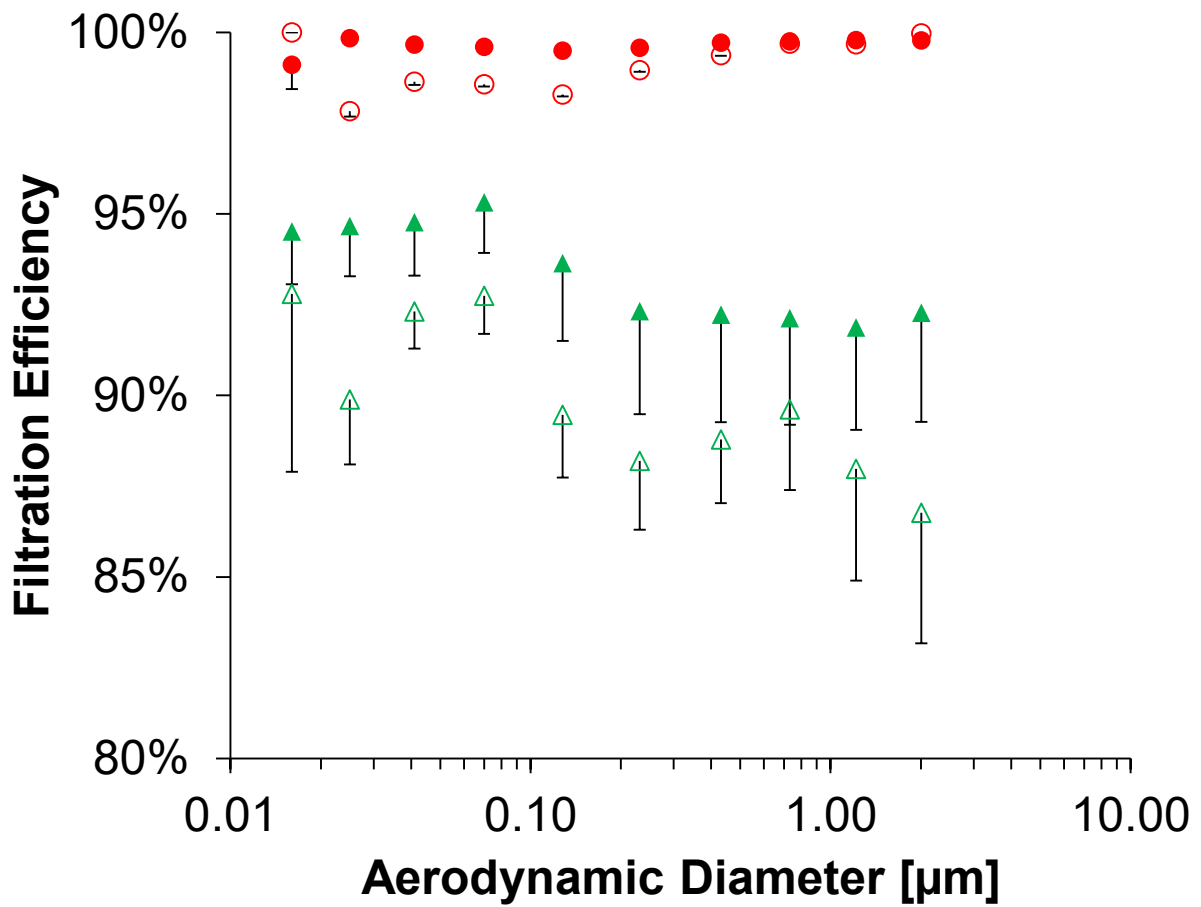
#### 1.13.4. Statistics

The open-source statistical program, JASP 0.14.1 (JASP, University of Amsterdam, Netherlands), was used to determine the statistical significance of differences and conduct post hoc studies. To check the statistically significant difference in FE at different face velocities and different particle sizes, a two-way mixed ANOVA was used with face velocity as a between-subjects factor and particle sizes as a repeated-measure factor. If there was a significant difference in FE between the adults' and children's face velocities, post hoc studies with Holm correction were conducted to determine which specific particle sizes were impacted by different face velocities. Holm correction was used because of the limited sample size (four per group) (Aickin & Gensler, 1996). To evaluate the impact of face velocity on pressure drops, two-way independent ANOVA was used with mask brand as the first independent factor, face velocity as the second independent factor, and pressure as a dependent factor. A confidence interval of 0.95 was used for all tests.

#### 1.14. Results

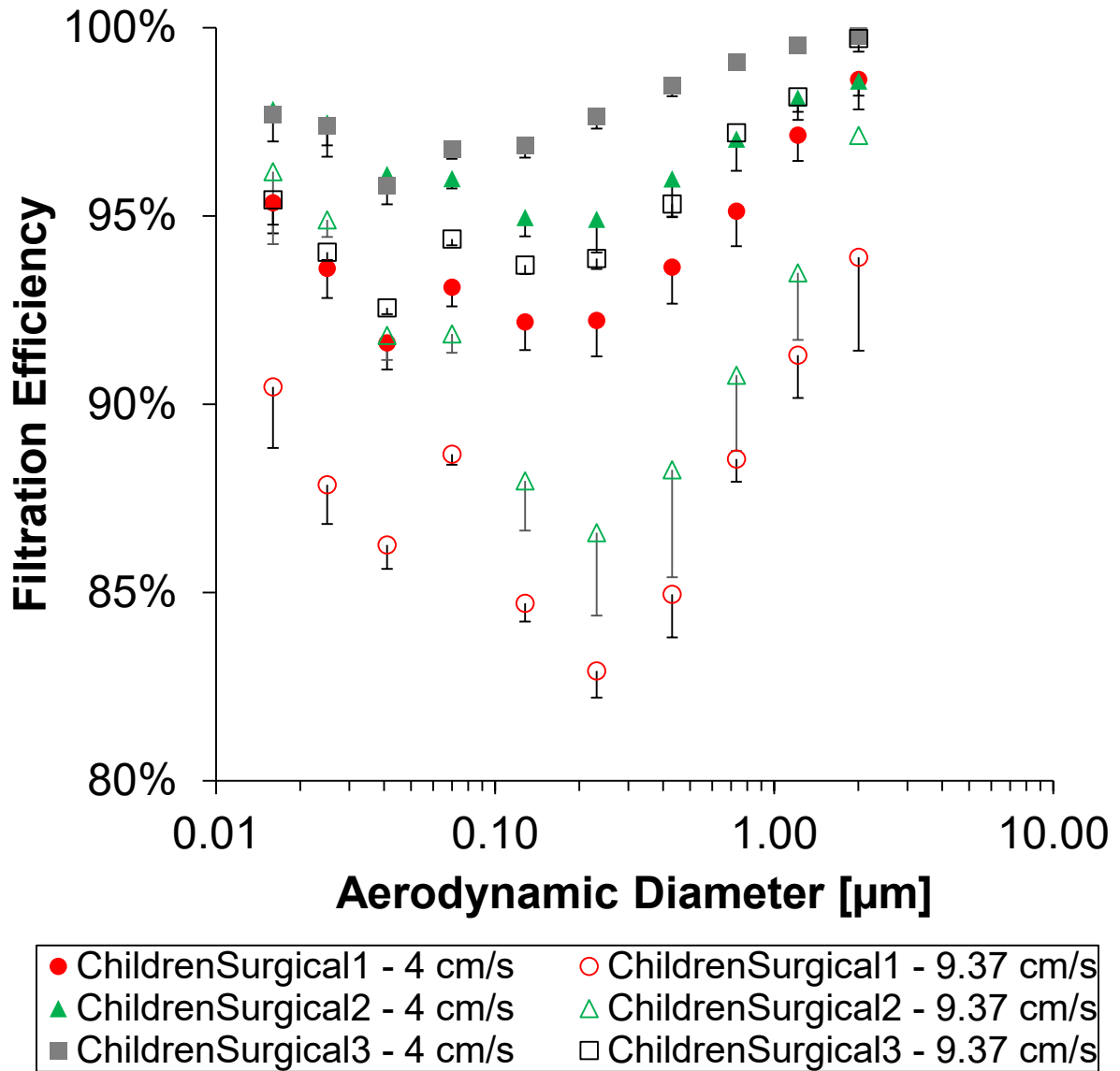
Size-specific FE of the five mask types at adult and children's face velocities are shown in Figure 4 - 2. Pressure drops at the two different face velocities and filter qualities calculated at minimum FE are tabulated in Table 4 - 3 and Table 4 - 4.





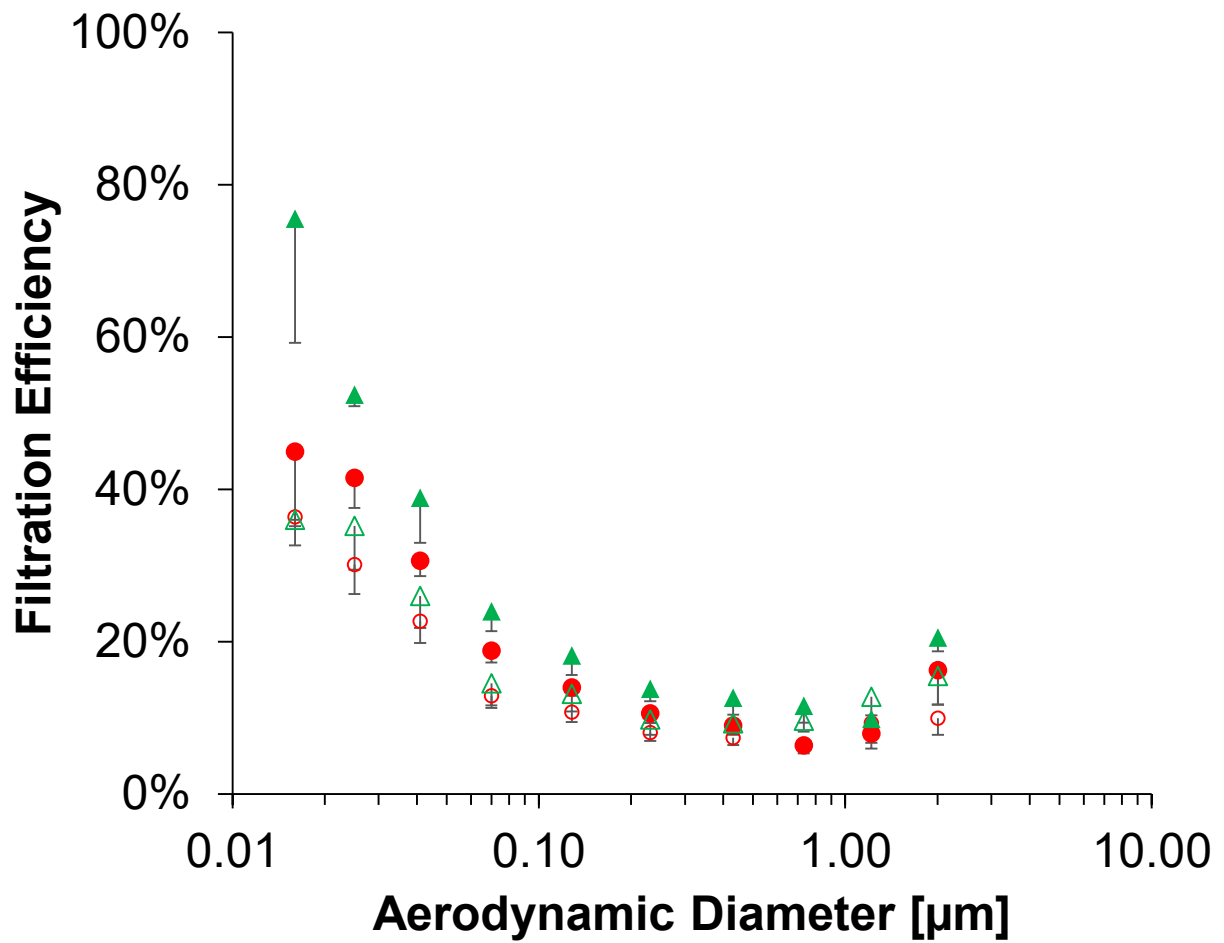
(a) Adult N95 and children KN95

Figure 4 - 2 Size-specific filtration efficiencies of the five mask types at two different face velocities



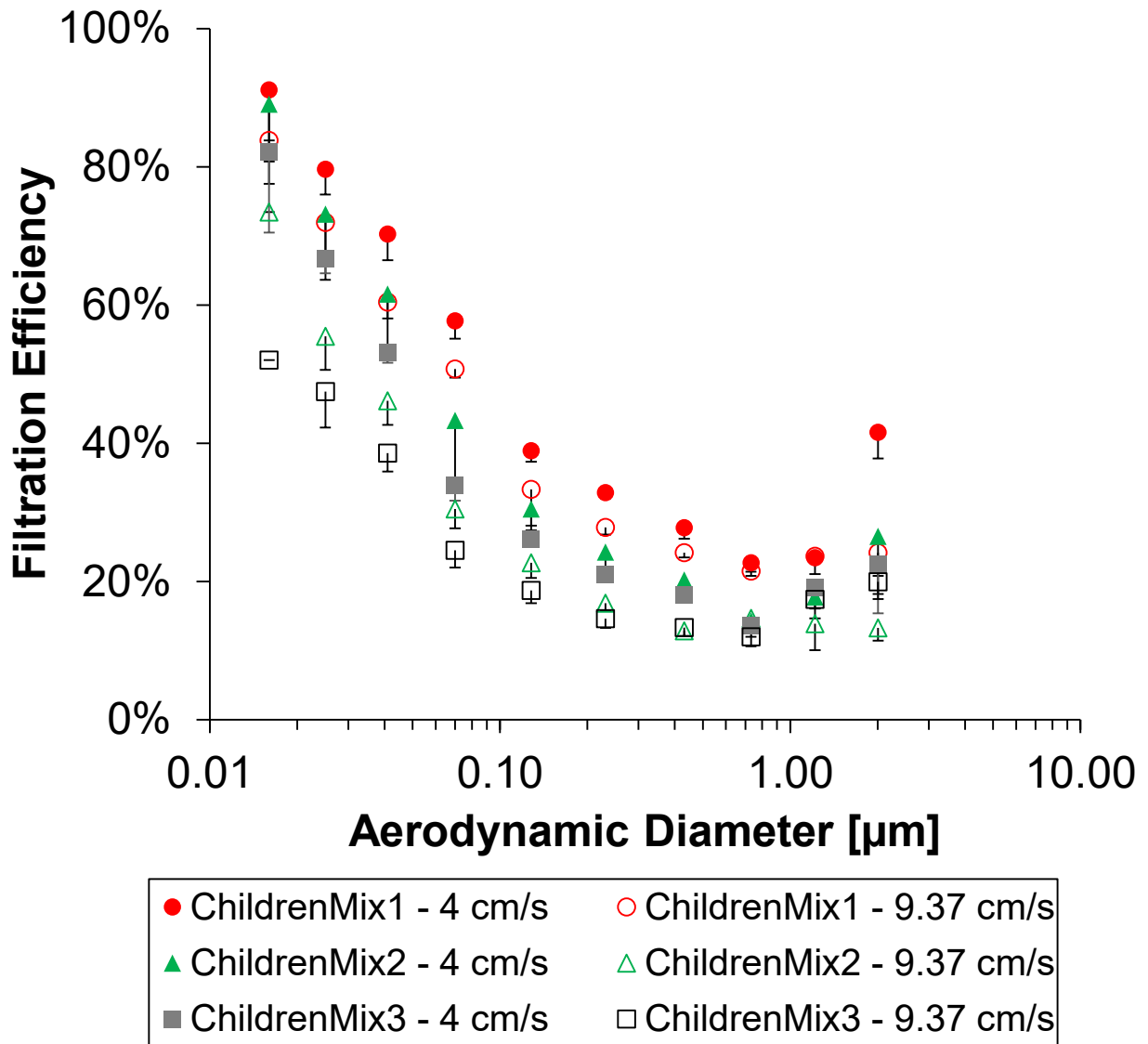
(b) Children Surgical

Figure 4 - 2 Size-specific filtration efficiencies of the five mask types at two different face velocities (continued)



(c) Children cotton

Figure 4 - 2 Size-specific filtration efficiencies of the five mask types at two different face velocities (continued)



(d) Children mixed materials

Figure 4 - 2 Size-specific filtration efficiencies of the five mask types at two different face velocities (continued)

At the high face velocity produced by an adult flow rate of 85 L/min, N95 masks maintained FEs consistently higher than 98%, while KN95 and surgical masks both averaged higher than 87%. Both cotton and mixed-material masks had a minimum FE between the aerodynamic diameter of 0.04  $\mu\text{m}$  and 0.07  $\mu\text{m}$ : cotton masks had an average minimum FE of 8% and mixed-material masks an FE of 16%. N95s exhibited the highest pressure drop of 133 Pa, while KN95 and surgical masks exhibited pressure drops similar to each other at 66 Pa and 76 Pa, respectively. Cotton and mixed-material masks also shared a similar level of pressure drop – 38 Pa and 37 Pa, respectively – which was the lowest of all the types tested. The trend of better performance in N95 and nonwoven masks was also highlighted in filter qualities. Using minimum filtration efficiencies, filter qualities were calculated as 29, 31, and 28  $\text{kPa}^{-1}$  respectively for N95, KN95, and surgical masks. Even though the N95 had a higher FE than KN95 and surgical masks, because of the N95's high pressure drop, N95 and other nonwoven masks had a similar filter quality. Due to lower FE, despite the lower pressure drop, woven masks had lower filter qualities: 2  $\text{kPa}^{-1}$  for cotton masks and 5  $\text{kPa}^{-1}$  for mixed-material masks.

At the low face velocity produced by the children's flow rate of approximately 33.7 L/min, the minimum FE went up to 99% for N95s, 92% for KN95s, and 94% on average for surgical masks. However, for cotton masks and mixed-material masks the minimum FE remained approximately the same at 8% and 17%, respectively. As pressure drop is directly proportional to face velocity (Hinds, 1999), pressure drop decreased by 2.3 times on average for all masks tested: at the low face velocity, N95s, KN95s, and surgical masks demonstrated pressure drops of 55, 33, and 31 Pa, respectively, while cotton masks and mixed-material masks demonstrated respective pressure drops of 18 and 16 Pa. As with pressure drop, filter qualities improved by more than two-fold. Surgical masks exhibited the highest filter quality at 91  $\text{kPa}^{-1}$ , while N95s and KN95s

exhibited similar filter qualities of 86 and 76  $\text{kPa}^{-1}$ , respectively. The filter qualities of cotton and mixed-material masks remained low at 5 and 12  $\text{kPa}^{-1}$ , respectively. Statistical tests, as detailed in the Method section, were conducted to determine if different face velocities made significant differences to FE and pressure drops. Results from statistical analyses to determine the significance of the changes in size-specific FE are listed in

Table 4 - 5. Two-way mixed ANOVA showed that testing FE at approximately 9.3 cm/s and 4.0 cm/s indicated significant differences for the adult N95 and all children's masks ( $p < 0.05$ ) except for the children's KN95 ( $p = 0.306$ ). Overall, both the adult N95 and KN95 showed relatively small differences in FE between the two face velocities (respectively, the maximum difference of 2.0% and 5.0% absolute). However, adult N95s had a narrow standard deviation of less than 1%, which likely led to statistical significance. For other masks, FEs were generally higher at the lower face velocity at every particle size. The post hoc tests showed that adults' N95 and surgical masks had significant differences in FE across most particle sizes tested, with significant changes in FE for particles in the range from 0.016 to 0.231  $\mu\text{m}$  for N95 and from 0.04 to 1.2  $\mu\text{m}$  for surgical masks. On the other hand, cotton and mixed-material masks experienced significant differences only in particle sizes smaller than 0.13  $\mu\text{m}$ , because, regardless of face velocities, FE at particle sizes larger than 0.13  $\mu\text{m}$  was consistently low for woven masks. At the lower face velocity, pressure drops were lowered by 2 to 2.5 times for all types of masks, and further ANOVA tests demonstrated that this difference in pressure drop between the low and high face velocity was statistically significant ( $p < 0.001$ ).

Table 4 - 3 Pressure drops and relative changes in filter quality for adult face velocity

<b>Adult Flow</b>				
<b>Mask Type</b>	<b>Min FE*</b>	<b>MPPS [<math>\mu\text{m}</math>] (min,max)</b>	<b>Pressure Drop [Pa]</b>	<b>qF at MPPS [kPa<sup>-1</sup>]</b>
<b>AdultN95</b>	97.8%	0.03	133 $\pm$ 8	29
<b>KN95</b>	86.8%	2.01	66 $\pm$ 7	31
<b>Surgical</b>	87.4 $\pm$ 4.9%	(0.04,0.23)	76 $\pm$ 13	27
<b>Cotton</b>	7.9 $\pm$ 2.0%	(0.43,0.73)	38 $\pm$ 14	2
<b>Mix</b>	15.5 $\pm$ 5.3%	(0.43,0.73)	37 $\pm$ 11	5

\*Average of minimum filtration efficiencies from all brands  $\pm$  standard deviation

Table 4 - 4 Pressure drops and relative changes in filter quality for children face velocity

<b>Children Flow</b>					
<b>Mask Type</b>	<b>Min FE</b>	<b>MPPS [<math>\mu\text{m}</math>] (min,max)</b>	<b>Pressure Drop [Pa]</b>	<b>qF at MPPS [kPa<sup>-1</sup>]</b>	<b>Relative Change in qF from Adult to Children Flow</b>
<b>AdultN95</b>	99.1%	0.02	55 $\pm$ 2	86	3.0x
<b>KN95</b>	91.9%	0.04	33 $\pm$ 9	76	2.5x
<b>Surgical</b>	94.1 $\pm$ 11.0%	(0.04,0.23)	31 $\pm$ 4	91	3.3x
<b>Cotton</b>	8.1 $\pm$ 2.5%	(0.73,1.22)	18 $\pm$ 8	5	2.2x
<b>Mix</b>	16.9 $\pm$ 5.1%	0.732	16 $\pm$ 4	12	2.5x

\*Average of minimum filtration efficiencies from all brands  $\pm$  standard deviation



Table 4 - 5 p-values from Holm test (95% confidence interval)

<b>D<sub>aero</sub> [μm]</b>	<b>Adult N95</b>	<b>Surgical 1</b>	<b>Surgical 2</b>	<b>Surgical 3</b>	<b>KN95</b>
0.016	<1E-3	<1E-3	1	<1E-3	N/A
0.025	<1E-3	<1E-3	0.966	<1E-3	
0.041	<1E-3	<1E-3	0.03	<1E-3	
0.070	<1E-3	0.045	0.039	<1E-3	
0.128	<1E-3	<1E-3	<1E-3	<1E-3	
0.231	<1E-3	<1E-3	<1E-3	<1E-3	
0.431	0.27	<1E-3	<1E-3	<1E-3	
0.732	1	<1E-3	<1E-3	<1E-3	
1.217	1	0.007	0.014	0.001	
2.007	1	0.026	1	1	

Note: Significant p-values are greyed.

Table 4 - 5 continued

<b>D<sub>aero</sub> [μm]</b>	<b>Cotton 1</b>	<b>Cotton 2</b>	<b>Mix 1</b>	<b>Mix 2</b>	<b>Mix 3</b>
0.016	0.036	<1E-3	0.367	0.013	<1E-3
0.025	<1E-3	<1E-3	0.259	0.003	<1E-3
0.041	0.079	0.032	0.029	0.014	<1E-3
0.070	0.775	0.562	0.499	0.091	0.047
0.128	1	1	1	1	0.422
0.231	1	1	1	1	1
0.431	1	1	1	1	1
0.732	1	1	1	1	1
1.217	1	1	1	1	1
2.007	0.525	1	1	0.069	1

## 1.15. Discussion

### 1.15.1. General Conclusion on Filtration Efficiency of N95, Surgical Masks, and Cloth-based Masks

Given that previous studies used different face velocities and test particles (Qian et al., 1998; Sankhyan et al., 2021), direct comparison with previous data was not possible. However, Qian et al (1998) found that at an 85 L/min flow rate with particle aerodynamic diameters from 0.1 to 1  $\mu\text{m}$ , N95s performed above 95% FE while surgical masks ranged from 70 to 80 % FE. Moreover, results from Sankhyan et al. (2021) showed that N95 masks demonstrated a filter quality range of 20 to 35  $\text{kPa}^{-1}$  at 85 L/min, surgical masks a comparable range of 15 to 35  $\text{kPa}^{-1}$ , and cloth masks the lowest range of 5 to 20  $\text{kPa}^{-1}$ . The general conclusion from other studies was that, in order of FE and filter quality, N95s ranked highest, closely followed by surgical masks and lastly by cloth-based masks, findings that align with those of the present study.

### 1.15.2. Effect of Face Velocity on Filtration Efficiency, Pressure Drop, and Filter Quality

This study assessed FE and pressure drop at a face velocity representative of children, and the results suggest that the filter materials of nonwoven masks marketed for children can provide FE higher than 90% for the intended population. Theoretically, it was expected that filtration through gravitational settling, diffusion, and electrostatic attraction would increase for the lower face velocity. According to single-fiber filtration theory, filtration by gravitational settling is inversely proportional to face velocity; filtration by diffusion is inversely proportional to (face velocity)<sup>2/3</sup>; and filtration by electrostatics is inversely proportional to (face velocity)<sup>1/2</sup> (Hinds, 1999). While filtration by impaction would theoretically have decreased with face velocity, the three mechanisms combined outweighed the effect of face velocity on impaction over the particle size range tested. All mask types in this experiment experienced an increase in FE for particle sizes

up to 0.07  $\mu\text{m}$  with the lower face velocity. This result also agrees with previous literature, which has demonstrated that a lower face velocity will result in higher FE due to increased diffusion and electrostatic effects for particle sizes smaller than 1  $\mu\text{m}$  (Huang et al., 2013) and electrostatic attraction for particle sizes between 0.1  $\mu\text{m}$  and 0.25  $\mu\text{m}$  (Martin & Moyer, 2000). It is notable that, unlike the N95, surgical masks often do not specify the inclusion of electret filters, but may nevertheless have benefited from electrostatic capture of particles by virtue of their construction including nonwoven materials (Drewnick et al., 2021). Furthermore, slightly better FE in mixed-material masks than in pure cotton masks may be attributable to polyester woven fabrics maintaining a greater static charge than natural fiber or cotton due to reduced absorption of water, and can thus boost FE from electrostatic effects (Tcharkhtchi et al., 2021).

Given the health risks associated with the inhalation of particles smaller than the aerodynamic diameter of 10  $\mu\text{m}$  (Xing et al., 2016), and given children's greater vulnerability to a smaller and wider range of particles (Brown et al., 2013), the results of size-specific FE testing in this experiment raise concerns about children's use of woven masks. The present study has shown that, even at a lower face velocity, cotton masks were able to provide FE over 50% only for particles smaller than 0.016  $\mu\text{m}$ . For mixed-material masks, FE over 50% was typically provided only for particles smaller than 0.04  $\mu\text{m}$ . Conversely, the minimum FE of over 92% for particles smaller than 2  $\mu\text{m}$  in children's surgical and KN95 masks verifies previous studies' conclusions about the superiority of nonwoven masks over woven masks (Tcharkhtchi et al., 2021). Based on this study, the results suggest that the use of woven masks alone to mitigate inhalation exposure could leave children unprotected against a window of particle sizes between 0.05 and 2  $\mu\text{m}$ , a finding of concern as particulates with diameters smaller than 2.5  $\mu\text{m}$  have been shown to present a graver health risk than larger particles because of larger specific surface areas and more distal

deposition in the respiratory tract (Xing et al., 2016; Xu et al., 2020). Such fine aerosols are also thought to contribute significantly to the spread of various diseases including SARS-CoV-2, with the microenvironment within bioaerosols allowing for longer pathogen lifetimes (Comunian et al., 2020). With a higher preference for cloth masks over respirators and surgical masks in this age group (Martin & Moyer, 2000), school-aged children may not be well protected against harmful aerosols, particularly in the absence of additional mitigating layers such as improved ventilation.

### 1.15.3. Limitations

In the present study, the number of masks and face velocities tested were limited. Future studies might employ different types of children's masks, as well as different compositions of mask materials. In regard to the effect of different face velocities, theoretically, with a lower face velocity the most penetrating particle size is expected to be smaller for masks that include electrostatic effects than for masks without electrostatic effects (Huang et al., 2013). It is likely that the two face velocities in this experiment were not drastically different enough to change the measured most penetrating particle size. Larger changes in face velocity representing, for instance, smaller children or children with restrictive lung disease could lead to a different result, and it would be of interest to apply a wider range of face velocities to understand the potential effect of different users on size-specific FE. Besides a lower minute volume, children also have higher breathing frequency, which was not accounted for with a constant flow rate in this experiment, and this would lead to a lower FE due to uneven distribution of air load over the area of the filter (Bazaluk et al., 2021). For example, under heavy exercise, the breathing frequency for a 5-year-old boy has been reported as 44 breaths per minute, while for a 30-year-old woman it has been reported as 33 breaths per minute (ICRP, 1994). While cyclic flow reflecting the different breathing frequencies could be approximated by choosing a constant flow rate between mean and

peak inhalation rate (Bahloul et al., 2014; Eshbaugh et al., 2008), the use of cyclic flow directly in future's in vitro studies could potentially influence measured FEs.

The effect of wash cycles or treatments for reuse, to which children's masks are often subjected, was also not investigated in this study. On one hand, some studies have suggested that the wash cycle does not influence FE: Sankhyan et al. (Sankhyan et al., 2021) found that up to 52 washer-dryer cycles did not impact the FE of the two-layer cotton coupon. On the other hand, Neupane et al. (Chua et al., 2020) found that PM<sub>10</sub> FE decreased by 20% after four washing and drying cycles in cloth masks possibly because of the increase in pore size and the lack of microfibers within the pore region. Given these conflicting findings, wash and dry cycles on children's masks should be applied with caution.

Lastly, the effects of mask fit on children were not measured in this experiment. In addition to the material FE, mask fit is crucial to ensuring containment and filtration of harmful aerosols (Tanisali et al., 2021). Oberg et al. (Oberg & Brosseau, 2008) found that surgical masks donned without assistance scored an average fit factor of 4.4, whereas respirators must achieve a fit factor of 100 to pass fit testing. Surgical masks with a loose fit could result in up to 40% penetration through face seal leakage compared to less than 10% penetration through the filter medium (Grinshpun et al., 2009). Given that children often experience inferior mask fit (Eberhart et al., 2021), any leakage from loose fit or additional fit modifications to a face mask (Blachere et al., 2022) should be explored in the future. Tight mask fit carries its own concerns, primarily with respect to tolerance and potential breathing discomfort. Further optimization of high-performance masks for use by children could potentially alleviate such concerns.

### 1.16. Conclusion

The performance of children's face masks in protecting against harmful aerosols has not been widely characterized. In this study, the size-specific FE and pressure drop were tested for an adult N95 (as control) and for children's KN95, surgical, cotton, and mixed-material masks using face velocities representative of children's versus adults' breathing patterns. It was observed that at the lower face velocity representative of children, FE typically increased for all particle sizes, except in woven masks for particle sizes larger than 0.1  $\mu\text{m}$ , in which FEs were consistently low for both adults' and children's face velocities. At the children's face velocity, nonwoven filter qualities were higher and ranged from 76 to 91  $\text{kPa}^{-1}$ , while woven masks had lower filter qualities ranging from 5 to 12  $\text{kPa}^{-1}$ . Supported by single-fiber filtration theory and previous literature, this study demonstrated that reducing face velocity to represent children's breathing patterns resulted in increased material FE and filter quality for nonwoven masks across the submicron and micron particle size range evaluated. Conversely, for woven masks, the FE for particles larger than 0.04  $\mu\text{m}$  was consistently low (typically < 50%) for both face velocities, with minimum FEs as low as 7.9% for cotton masks, and 15.5% for mixed-material masks.

## Chapter 5 Conclusion

### 1.17. Summary

The FE and pressure drops of masks have been actively researched, especially through respiratory disease pandemics, but the capacity of masks is difficult to define as it is often limited by manufacturability and influenced by various intrinsic and external factors. Furthermore, masks are regulated by organizations such as NIOSH and FDA in the United States but the test scenario in their evaluations is limited in terms of test particle sizes and flow rates despite vast variations in users and usage environments. To expand the database on the FE of constantly-evolving masks, the objectives of this thesis were to examine the effects of two commonly discussed external modifications – repeated cycles of decontaminations and children’s flow rate – by measuring size-specific FE and pressure drops in a custom experiment set-up with an ELPI.

In Chapter 3, FE and pressure drops of two different N95 respirators were compared before and after ten cycles of moist heat incubation decontaminations, and it was shown that it can significantly decrease FE, likely due to decreased electrostatic effect. The usage of an ELPI in the experiment also showed that the NIOSH’s range of test particles may not be sufficient to represent the minimum FE, especially after decontamination such as moist heat incubation through high temperature and humidity. NIOSH’s test particles range (aerodynamic diameters between 0.06  $\mu\text{m}$  to 0.21  $\mu\text{m}$ ) targets to measure FE at the most penetrating particle size for typical respirators with electrets, yet the electrostatic effect is applicable up to 1  $\mu\text{m}$  (Huang et al., 2013) hence the minimum FE measured outside of the NIOSH’s test particle size demonstrated the need to use a wider size range for test particles.

Chapter 4 further utilized the modified experiment set-up from Chapter 3 and children’s KN95, surgical, cotton, and mixed-material masks to show that school-aged children as mask users

can have higher FE, lower pressure drops, and consequently higher filter quality than adults due to their lower flow rate. It also emphasized that woven masks' material FE for particle sizes larger than 0.04  $\mu\text{m}$  is less than nonwoven masks' regardless of flow rate, which could expose the users unprotected against a window of particle sizes between 0.05 and 2  $\mu\text{m}$ .

The research in this thesis provides information on the masks' performance through various means including SEM imaging and size-specific FE, which can help users to make an objective judgment. It also emphasizes the need for a more expansive test than the current "gold" standard NIOSH's test to include contexts besides industrial settings and to consider populations including pediatric and potentially other populations with different lung capacities compared to typical adults. This research can hopefully be used to develop a more realistic FE test and to develop better masks by better understanding the effect of external factors.

#### 1.18. Future Work

Expanding upon the decontamination study in Chapter 3, other commonly used decontamination methods or wash cycles can degrade the material and should be studied further. Furthermore, particulate matters can act as "cargos" and increase the danger of transmitting diseases like SARS-CoV-2 (Paital & Agrawal, 2022), and different types of particulates have different levels of toxicity. Instead of purely looking at FE, looking at dosage (e.g., the mass of viruses that users are exposed to) might be helpful from the perspective of health sciences.

Expanding upon the children's masks study in Chapter 4, the effect of a wider range of different face velocities should be investigated. A higher velocity theoretically would decrease FE, and the direct measurement of FE would be helpful for those who breathe at a higher volume rate. For example, for restrictive lungs from diseases, the deposited dose is generally higher in subjects with lung problems (Hussein et al., 2013), and they have higher breathing rates (Monjezi &



Jamaati, 2021) and potentially irregular breathing patterns which can increase impaction from cyclic breathing and consequently lower FE of the masks.

As discussed in both Chapters 3 and 4, FE alone is not the conclusive performance benchmark as leakage could be significant if not fitted properly, and a realistic FE when donned can be much lower. Knowing that the trends of size-specific FE differ by mask type, a size-specific fit test could be interesting to further improve the seal of the masks. Furthermore, masks may be worn to protect the wearer from inhaled aerosols but, at the same time, may also capture the wearer's exhaled aerosols, thereby potentially limiting transmission of airborne pathogens to others. Measuring the mask's filtration efficiency in the latter case may require different test particle conditions. Note that this study's results directly apply to the FE when protecting the mask wearer from incoming aerosols. While the test particles in this thesis were dried, aerosols contained in exhaled air likely contain higher water content, and may exist as larger droplets traveling at higher velocities (e.g. during coughing, sneezing, or speech), when they interact with masks.

This thesis focuses mostly on the performance of the masks but, to enforce the usage of the masks, comfort should be considered and quantified. For example, Mojezi et al. (2021) utilized the work of breathing for normal, restrictive, and obstructive-lung-conditioned groups to quantify the potential added discomfort to users with pre-existing lung conditions (Monjezi & Jamaati, 2021). Intrinsic characteristics of masks such as material, TPI, and mean fiber diameter could also be specified in future studies so that a clearer relationship between intrinsic and external factors could be directly related, rather than, for example, generalizing performance of the two broad types, woven and nonwoven. Lastly, more realistic situations like longer usage of masks through such as loading study (Forouzandeh et al., 2021; Guha et al., 2015) or elevated activity level should be studied along with fit as the fit is prone to change throughout activities.

## Works Cited

- 3M. (2021). *Comparison Of FFP2 , KN95 , And N95 Filtering Facepiece Respirator Classes 3M Personal Safety Division*. <https://multimedia.3m.com/mws/media/1791500O/comparison-ffp2-kn95-n95-filtering-facepiece-respirator-classes-tb.pdf> . Accessed November 6, 2022.
- Adanur, S., & Jayswal, A. (2020). Filtration Mechanisms And Manufacturing Methods Of Face Masks: An Overview. *Journal of Industrial Textiles*, 51(3S), 3683S-3717S. DOI:10.1177/1528083720980169
- Ahmad, M. D. F., Wahab, S., Ali Ahmad, F., Intakhab Alam, M., Ather, H., Siddiqua, A., Amir Ashraf, S., Abu Shaphe, M., Idreesh Khan, M., & Ali Beg, R. (2021). A Novel Perspective Approach To Explore Pros And Cons Of Face Mask In Prevention The Spread Of SARS-CoV-2 And Other Pathogens. *Saudi Pharmaceutical Journal*, 29(2), 121–133. DOI:10.1016/j.jsps.2020.12.014
- Aickin, M., & Gensler, H. (1996). Adjusting For Multiple Testing When Reporting Research Results: The Bonferroni vs Holm Methods. *American Journal of Public Health*, 86(5), 726–728. DOI:10.2105/AJPH.86.5.726
- Bahloul, A., Mahdavi, A., Haghghat, F., & Ostiguy, C. (2014). Evaluation Of N95 Filtering Facepiece Respirator Efficiency With Cyclic And Constant Flows. *Journal of Occupational and Environmental Hygiene*, 11(8), 499–508. DOI:10.1080/15459624.2013.877590
- Bar-On, Y. M., Flamholz, A., Phillips, R., & Milo, R. (2020). SARS-CoV-2 (COVID-19) by the numbers. *ELife*, 9, e57309. DOI:10.7554/eLife.57309
- Bazaluk, O., Ennan, A., Cheberichko, S., Deryugin, O., Cheberichko, Y., Saik, P., Lozynskyi, V., & Knysh, I. (2021). Research On Regularities Of Cyclic Air Motion Through A Respirator Filter. *Applied Sciences (Switzerland)*, 11(7), 3157. DOI:10.3390/app11073157

- Bergman, M. S., Viscusi, D. J., Heimbuch, B. K., Wander, J. D., Sambol, A. R., & Shaffer, R. E. (2010). Evaluation Of Multiple (3-cycle) Decontamination Processing For Filtering Facepiece Respirators. *Journal of Engineered Fibers and Fabrics*, 5(4), 33–41. DOI:10.1177/155892501000500405
- Bergman, M. S., Viscusi, D. J., Palmiero, A. J., Powell, J. B., & Shaffer, R. E. (2011). Impact of Three Cycles Of Decontamination Treatments On Filtering Facepiece Respirator Fit. *Journal of the International Society for Respiratory Protection*, 28(1), 48–59.
- Blachere, F. M., Lemons, A. R., Coyle, J. P., Derk, R. C., Lindsley, W. G., Beezhold, D. H., Woodfork, K., Duling, M. G., Boutin, B., Boots, T., Harris, J. R., Nurkiewicz, T., & Noti, J. D. (2022). Face Mask Fit Modifications That Improve Source Control Performance. *American Journal of Infection Control*, 50(2), 133–140. DOI:10.1016/j.ajic.2021.10.041
- Brosseau, L. M., & Shaffer, R. (2014). *Do We Need to Challenge Respirator Filters With Biological Aerosols?* NIOSH Science Blog Safer Healthier Workers. <http://blogs.cdc.gov/niosh-science-blog/2014/04/02/respirator-filter-testing/> . Accessed November 6, 2022.
- Brown, J. S., Gordon, T., Price, O., & Asgharian, B. (2013). Thoracic And Respirable Particle Definitions For Human Health Risk Assessment. *Particle and Fibre Toxicology*, 10(1), 1–12. DOI:10.1186/1743-8977-10-12
- CDC. (2020). *Implementing Filtering Facepiece Respirator (FFR) Reuse, Including Reuse after Decontamination, When There Are Known Shortages of N95 Respirators.* <https://www.cdc.gov/coronavirus/2019-ncov/hcp/ppe-strategy/decontamination-reuse-respirators.html> . Accessed January 4, 2020.
- ChineseStandard.net. (n.d). GB 2626-2006.

<https://www.chinesestandard.net/PDF/English.aspx/GB2626-2006> . Accessed August 15, 2022.

Chua, M. H., Cheng, W., Goh, S. S., Kong, J., Li, B., Lim, J. Y. C., Mao, L., Wang, S., Xue, K., Yang, L., Ye, E., Zhang, K., Cheong, W. C. D., Tan, B. H., Li, Z., Tan, B. H., & Loh, X. J. (2020). Face Masks In The New COVID-19 Normal: Materials, Testing, And Perspectives. *Research*, 2020, 1–40. DOI:10.34133/2020/7286735

Clase, C. M., Fu, E. L., Ashur, A., Beale, R. C. L., Clase, I. A., Dolovich, M. B., Jardine, M. J., Joseph, M., Kansime, G., Mann, J. F. E., Pecoits-Filho, R., Winkelmayr, W. C., & Carrero, J. J. (2020). Forgotten Technology In The COVID-19 Pandemic: Filtration Properties Of Cloth And Cloth Masks—A Narrative Review. *Mayo Clinic Proceedings*, 95(10), 2204–2224. DOI:10.1016/j.mayocp.2020.07.020

Comunian, S., Dongo, D., Milani, C., & Palestini, P. (2020). Air Pollution And Covid-19: The Role Of Particulate Matter In The Spread And Increase Of Covid-19's Morbidity And Mortality. *International Journal of Environmental Research and Public Health*, 17(12), 1–22. DOI:10.3390/ijerph17124487

Daeschler, S. C., Manson, N., Joachim, K., Chin, A. W. H., Chan, K., Chen, P. Z., Tajdaran, K., Mirmoeini, K., Zhang, J. J., Maynes, J. T., Zhang, L., Science, M., Darbandi, A., Stephens, D., Gu, F., Poon, L. L. M., & Borschel, G. H. (2020). Effect Of Moist Heat Reprocessing Of N95 Respirators On SARS-CoV-2 Inactivation And Respirator Function. *CMAJ*, 192(41). DOI:10.1503/cmaj.201203

Dekati Ltd. (2018). *Dekati ELPI+ User Manual Ver. 1.55*.

Drewnick, F., Pikkmann, J., Fehlinger, F., Moormann, L., Sprang, F., & Borrmann, S. (2021). Aerosol Filtration Efficiency Of Household Materials For Homemade Face Masks: Influence

- Of Material Properties, Particle Size, Particle Electrical Charge, Face Velocity, And Leaks. *Aerosol Science and Technology*, 55(1), 63–79. DOI:10.1080/02786826.2020.1817846
- Eberhart, M., Orthaber, S., & Kerbl, R. (2021). The Impact Of Face Masks On Children: A Mini Review. *Acta Paediatrica, International Journal of Paediatrics*, 110(6), 1778–1783. DOI:10.1111/apa.15784
- Encycl. (n.d.). *KF94 (/ KF94 )*. <https://encycla.com/KF94> . Accessed November 6, 2022.
- Eninger, R. M., Honda, T., Reponen, T., McKay, R., & Grinshpun, S. A. (2008). What Does Respirator Certification Tell Us About Filtration Of Ultrafine Particles? *Journal of Occupational and Environmental Hygiene*, 5(5), 286–295. DOI:10.1080/15459620801960153
- Eshbaugh, J. P., Gardner, P. D., Richardson, A. W., & Hofacre, K. C. (2008). N95 And P100 Respirator Filter Efficiency Under High Constant And Cyclic Flow. *Journal of Occupational and Environmental Hygiene*, 6(1), 52–61. DOI:10.1080/15459620802558196
- Fairbrother, R. W. (1945). The Destruction Of Bacteria. In *A Text-Book of Bacteriology* (4th ed., pp. 53–64). William Heinemann Medical Books Ltd.
- FDA. (2004). Guidance For Industry And FDA Staff: Surgical Masks - Premarket Notification [510 (k)] Submissions. *Fda.Gov*, 510, 14. <https://www.fda.gov/regulatory-information/search-fda-guidance-documents/surgical-masks-premarket-notification-510k-submissions>
- Finlay, W. H. (2019). Motion Of A Single Aerosol Particle In A Fluid. In *The Mechanics of Inhaled Pharmaceutical Aerosols* (2nd ed., pp. 21–52). Mara Conner Acquisition. DOI:10.1016/b978-0-08-102749-3.00003-8
- Fisher, E. M., Williams, J. L., & Shaffer, R. E. (2011). Evaluation Of Microwave Steam Bags For

- The Decontamination Of Filtering Facepiece Respirators. *PLoS ONE*, 6(4), e18585.  
DOI:10.1371/journal.pone.0018585
- Forouzandeh, P., O'Dowd, K., & Pillai, S. C. (2021). Face Masks And Respirators In The Fight Against The COVID-19 Pandemic: An Overview Of The Standards And Testing Methods. *Safety Science*, 133, 104995. DOI:10.1016/j.ssci.2020.104995
- Golshahi, L., Noga, M. L., Thompson, R. B., & Finlay, W. H. (2011). In Vitro Deposition Measurement Of Inhaled Micrometer-sized Particles In Extrathoracic Airways Of Children And Adolescents During Nose Breathing. *Journal of Aerosol Science*, 42(7), 474–488. DOI:10.1016/j.jaerosci.2011.04.002
- Gong, H., & Ozgen, B. (2017). Fabric Structures: Woven, Knitted, Or Nonwoven. In *Engineering of High-Performance Textiles*. Elsevier Ltd. DOI:10.1016/B978-0-08-101273-4.00007-X
- Grinshpun, S. A., Haruta, H., Eninger, R. M., Reponen, T., McKay, R. T., & Lee, S. A. (2009). Performance Of An N95 Filtering Facepiece Particulate Respirator And A Surgical Mask During Human Breathing: Two Pathways For Particle Penetration. *Journal of Occupational and Environmental Hygiene*, 6(10), 593–603. DOI:10.1080/15459620903120086
- Guha, S., Mejía-Alfaro, A., Hariharan, P., & Myers, M. R. (2015). Effectiveness Of Facemasks For Pediatric Populations Against Submicron-sized Aerosols. *American Journal of Infection Control*, 43(8), 871–877. DOI:10.1016/j.ajic.2015.03.032
- Hao, W., Parasch, A., Williams, S., Li, J., Ma, H., Burken, J., & Wang, Y. (2020). Filtration Performances Of Non-medical Materials As Candidates For Manufacturing Facemasks And Respirators. *International Journal of Hygiene and Environmental Health*, 229, 113582. DOI:10.1016/j.ijheh.2020.113582
- He, X., Reponen, T., McKay, R. T., & Grinshpun, S. A. (2013). Effect Of Particle Size On The

- Performance Of An N95 Filtering Facepiece Respirator And A Surgical Mask At Various Breathing Conditions. *Aerosol Science and Technology*, 47(11), 1180–1187. DOI:10.1080/02786826.2013.829209
- Heimbuch, B. K., Wallace, W. H., Kinney, K., Lumley, A. E., Wu, C. Y., Woo, M. H., & Wander, J. D. (2011). A Pandemic Influenza Preparedness Study: Use of Energetic Methods To Decontaminate Filtering Facepiece Respirators Contaminated With H1N1 Aerosols And Droplets. *American Journal of Infection Control*, 39(1), e1–e9. DOI:10.1016/j.ajic.2010.07.004
- Hinds, W. C. (1999). Filtration. In *Aerosol Technology: Properties, Behavior, And Measurement Of Airborne Particles* (2nd ed., pp. 182–205). Wiley.
- Hofmann, W. (2011). Modelling Inhaled Particle Deposition In The Human Lung: A Review. *Journal of Aerosol Science*, 42(10), 693–724. DOI:10.1016/j.jaerosci.2011.05.007
- Howard, J., Huang, A., Li, Z., Tufekci, Z., Zdimas, V., van der Westhuizen, H. M., von Delft, A., Price, A., Fridman, L., Tang, L. H., Tang, V., Watson, G. L., Bax, C. E., Shaikh, R., Questier, F., Hernandez, D., Chu, L. F., Ramirez, C. M., & Rimoin, A. W. (2021). An Evidence Review Of Face Masks Against COVID-19. *Proceedings of the National Academy of Sciences of the United States of America*, 118(4), 1–12. DOI:10.1073/pnas.2014564118
- Huang, S. H., Chen, C. W., Kuo, Y. M., Lai, C. Y., McKay, R., & Chen, C. C. (2013). Factors Affecting Filter Penetration And Quality Factor Of Particulate Respirators. *Aerosol and Air Quality Research*, 13(1), 162–171. DOI:10.4209/aaqr.2012.07.0179
- Hussein, T., Löndahl, J., Paasonen, P., Koivisto, A. J., Petäjä, T., Hämeri, K., & Kulmala, M. (2013). Modeling Regional Deposited Dose Of Submicron Aerosol Particles. *Science of the Total Environment*, 458–460, 140–149. DOI:10.1016/j.scitotenv.2013.04.022

- Hutten, I. M. (2007). Introduction To Nonwoven Filter Media. In *Handbook of Nonwoven Filter Media*. DOI:10.1016/b978-185617441-1/50016-0
- ICRP. (1994). *Human Respiratory Tract Model For Radiological Protection Vol. 24*.
- Janssen, L., Anderson, N., Weber, R., Cassidy, P., & Nelson, T. (2005). Interpretation Of Inhalation Airflow Measurements For Respirator Design And Testing. *Journal of the International Society for Respiratory Protection*, 22, 122–141. DOI:10.3320/1.2753437
- Järvinen, A., Aitomaa, M., Rostedt, A., Keskinen, J., & Yli-Ojanperä, J. (2014). Calibration Of The New Electrical Low Pressure Impactor (ELPI+). *Journal of Aerosol Science*, 69, 150–159. DOI:10.1016/j.jaerosci.2013.12.006
- Ju, J. T. J., Boisvert, L. N., & Zuo, Y. Y. (2021). Face Masks Against COVID-19: Standards, Efficacy, Testing And Decontamination Methods. *Advances in Colloid and Interface Science*, 292, 102435. DOI:10.1016/j.cis.2021.102435
- Kilic, A., Russell, S., Shim, E., & Pourdeyhimi, B. (2017). The Charging And Stability Of Electret Filters. In *Fibrous Filter Media* (pp. 95–121). Elsevier Inc. DOI:10.1016/B978-0-08-100573-6.00025-3
- Konda, A., Prakash, A., Moss, G. A., Schmoltdt, M., Grant, G. D., & Guha, S. (2020). Aerosol Filtration Efficiency of Common Fabrics Used in Respiratory Cloth Masks. *ACS Nano*, 14(5), 6339–6347. DOI:10.1021/acsnano.0c03252
- Li, L., Zuo, Z., Japuntich, D. A., & Pui, D. Y. H. (2012). Evaluation Of Filter Media For Particle Number, Surface Area And Mass Penetrations. *Annals of Occupational Hygiene*, 56(5), 581–594. DOI:10.1093/anhyg/mes034
- Liao, L., Xiao, W., Zhao, M., Yu, X., Wang, H., Wang, Q., Chu, S., & Cui, Y. (2020). Can N95 Respirators Be Reused After Disinfection? How Many Times? *ACS Nano*, 14(5).



DOI:10.1021/acsnano.0c03597

Liao, M., Liu, H., Wang, X., Hu, X., Huang, Y., Liu, X., Brennan, K., Mecha, J., Nirmalan, M., & Lu, J. R. (2021). A Technical Review Of Face Mask Wearing In Preventing Respiratory COVID-19 Transmission. *Current Opinion in Colloid and Interface Science*, 52, 101417. DOI:10.1016/j.cocis.2021.101417

Licina, A., & Silvers, A. (2021). Use Of Powered Air-purifying Respirator (PAPR) As Part Of Protective Equipment Against SARS-CoV-2 - A Narrative Review And Critical Appraisal Of Evidence. *American Journal of Infection Control*, 49(4), 492–499. DOI:10.1016/j.ajic.2020.11.009

Locke, L., Dada, O., & Shedd, J. S. (2021). Aerosol Transmission Of Infectious Disease And The Efficacy Of Personal Protective Equipment (PPE): A Systematic Review. *Journal of Occupational and Environmental Medicine*, 63(11), e783–e791. DOI:10.1097/JOM.0000000000002366

Lore, M. B., Heimbuch, B. K., Brown, T. L., Wander, J. D., & Hinrichs, S. H. (2012). Effectiveness Of Three Decontamination Treatments Against Influenza Virus Applied To Filtering Facepiece Respirators. *Annals of Occupational Hygiene*, 56(1), 92–101. DOI:10.1093/annhyg/mer054

Mahdavi, A., Haghghat, F., Bahloul, A., Brochot, C., & Ostiguy, C. (2015). Particle Loading Time And Humidity Effects On The Efficiency Of An N95 Filtering Facepiece Respirator Model Under Constant And Inhalation Cyclic Flows. *Annals of Occupational Hygiene*, 59(5), 629–640. DOI:10.1093/annhyg/mev005

Mao, J., Grgic, B., Finlay, W. H., Kadla, J. F., & Kerekes, R. J. (2008). Wood Pulp Based Filters For Removal Of Sub-micrometer Aerosol Particles. *Nordic Pulp and Paper Research*

- Journal*, 23(4), 420–425. DOI:10.3183/npprj-2008-23-04-p420-425
- Marr, L. C., Tang, J. W., Van Mullekom, J., & Lakdawala, S. S. (2019). Mechanistic Insights Into The Effect Of Humidity On Airborne Influenza Virus Survival, Transmission And Incidence. *Journal of the Royal Society Interface*, 16(150), 20180298. DOI:10.1098/rsif.2018.0298
- Martin, S. B., & Moyer, E. S. (2000). Electrostatic Respirator Filter Media: Filter Efficiency And Most Penetrating Particle Size Effects. *Applied Occupational and Environmental Hygiene*, 15(8), 609–617. DOI:10.1080/10473220050075617
- Monjezi, M., & Jamaati, H. (2021). The effects of face mask specifications on work of breathing and particle filtration efficiency. *Medical Engineering and Physics*, 98(October), 36–43. DOI:10.1016/j.medengphy.2021.10.004
- Moyer, Ernest S.; Stevens, G. A. (1989). “Worst Case” Aerosol Testing Parameters: II. Efficiency Dependence Of Commercial Respirator Filters On Humidity Pretreatment. *American Industrial Hygiene Association Journal*, 50(5). DOI:10.1080/15298668991374624
- Moyer, E. S., & Bergman, M. S. (2000). Electrostatic N-95 Respirator Filter Media Efficiency Degradation Resulting From Intermittent Sodium Chloride Aerosol Exposure. *Applied Occupational and Environmental Hygiene*, 15(8), 600–608. DOI:10.1080/10473220050075608
- Mueller, W., Horwell, C. J., Apsley, A., Steinle, S., McPherson, S., Cherrie, J. W., & Galea, K. S. (2018). The Effectiveness Of Respiratory Protection Worn By Communities To Protect From Volcanic Ash Inhalation: Part I Filtration Efficiency Tests. *International Journal of Hygiene and Environmental Health*, 221(6), 967–976. DOI:10.1016/j.ijheh.2018.03.012
- NPPTL. (2018). *100 Years Of Respiratory Protection History*. <https://www.cdc.gov/niosh/npptl/Respiratory-Protection-history.html> . Accessed August 10,

2022.

NPPTL. (2020a). *NPPTL Respirator Assessments To Support The COVID-19 Response: Beyond Shelf Life/Stockpiled Assessment Results.*

<https://www.cdc.gov/niosh/npptl/respirators/testing/ExpiredN95results.html> . Accessed January 5, 2021.

NPPTL. (2020b). *NPPTL Respirator Assessments To Support The COVID-19 Response: Decontaminated Assessment Results.*

<https://www.cdc.gov/niosh/npptl/respirators/testing/DeconResults.html> . Accessed January 4, 2021.

Oberg, T., & Brosseau, L. M. (2008). Surgical Mask Filter And Fit Performance. *American Journal of Infection Control*, 36(4), 276–282. DOI:10.1016/j.ajic.2007.07.008

OSHA. (2020). *Enforcement Guidance for Use of Respiratory Protection Equipment Certified under Standards of Other Countries or Jurisdictions During the Coronavirus Disease 2019 (COVID-19) Pandemic.* <https://www.osha.gov/memos/2020-04-03/enforcement-guidance-use-respiratory-protection-equipment-certified-under> . Accessed January 4, 2021.

Ou, Q., Pei, C., Chan Kim, S., Abell, E., & Pui, D. Y. H. (2020). Evaluation Of Decontamination Methods For Commercial And Alternative Respirator And Mask Materials – View From Filtration Aspect. *Journal of Aerosol Science*, 150, 105609. DOI:10.1016/j.jaerosci.2020.105609

Paital, B., & Agrawal, P. K. (2022). Role Of Environmental Factors In Transmission Of COVID-19. In *COVID-19 in the Environment* (Issue December 2020, pp. 35–72). Elsevier Inc. DOI:10.1016/b978-0-323-90272-4.00017-8

Qian, Y., Willeke, K., Grinshpun, S. A., Donnelly, J., & Coffey, C. C. (1998). Performance Of

- N95 Respirators: Filtration Efficiency For Airborne Microbial And Inert Particles. *American Industrial Hygiene Association Journal*, 59(2), 128–132. DOI:10.1080/15428119891010389
- Rengasamy, S., Eimer, B., & Shaffer, R. E. (2010). Simple Respiratory Protection - Evaluation Of The Filtration Performance Of Cloth Masks And Common Fabric Materials Against 20-1000 nm Size Particles. *Annals of Occupational Hygiene*, 54(7), 789–798. DOI:10.1093/annhyg/meq044
- Rengasamy, S., Miller, A., Eimer, B. C., & Shaffer, R. E. (2020). Filtration Performance Of FDA-Cleared Surgical Masks. *Journal of the International Society for Respiratory Protection*, 26(3), 54–70.
- Rengasamy, S., Shaffer, R., Williams, B., & Smit, S. (2017). A Comparison Of Facemask And Respirator Filtration Test Methods. *Journal of Occupational and Environmental Hygiene*, 14(2). DOI:10.1080/15459624.2016.1225157
- Rivers, R. D., & Murphy, D. J. (2000). Air Filter Performance Under Variable Air Volume Conditions. *ASHRAE Transactions*, 106.
- Rockwood, C. A. , O'Donoghue, D. H. (1960). The Surgical Mask: Its Development, Usage, And Efficiency. *A.M.A Archives of Surgery*, 80, 103–111.
- Roy, Monique. Courtay, C. (1991). Daily Activities and Breathing Parameters for Use in Respiratory Tract Dosimetry. *Radiation Protection Dosimetry*, 35(3), 179–186.
- Sankhyan, S., Heinselman, K. N., Ciesielski, P. N., Barnes, T., Himmel, M. E., Teed, H., Patel, S., & Vance, M. E. (2021). Filtration Performance Of Layering Masks And Face Coverings And The Reusability Of Cotton Masks After Repeated Washing And Drying. *Aerosol and Air Quality Research*, 21(11), 1–13. DOI:10.4209/AAQR.210117
- Scheepers, P. T. J., Wertheim, H. F. L., van Dael, M., Anzion, R., Holterman, H. J., Teerenstra,

- S., de Groot, M., Voss, A., & Hopman, J. (2021). Comparative Performance Testing Of Respirator Versus Surgical Mask Using A Water Droplet Spray Model. *International Journal of Environmental Research and Public Health*, 18(4), 1–9. DOI:10.3390/ijerph18041599
- Seo, S., Ruzycki, C. A., Johnson, B., Wang, H., Vehring, R., Romanyk, D., Finlay, W. H., & Martin, A. R. (2022). Size-Specific Filtration Performance Of N95 Respirators After Decontamination By Moist Heat Incubation. *Journal of Aerosol Medicine and Pulmonary Drug Delivery*, 35(1), 41–49. DOI:10.1089/jamp.2021.0002
- Sipkens, T. A., Corbin, J. C., Koukoulas, T., Oldershaw, A., Lavoie, T., Norooz Oliaee, J., Liu, F., Leroux, I. D., Smallwood, G. J., Lobo, P., & Green, R. G. (2022). Comparison Of Measurement Systems For Assessing Number- And Mass-based Particle Filtration Efficiency. *Journal of Occupational and Environmental Hygiene*, 19(10–11), 629–645. DOI:10.1080/15459624.2022.2114596
- Steinberg, B. E., Aoyama, K., McVey, M., Levin, D., Siddiqui, A., Munshey, F., Goldenberg, N. M., Faraoni, D., & Maynes, J. T. (2020). Efficacy And Safety Of Decontamination For N95 Respirator Reuse: A Systematic Literature Search And Narrative Synthesis. *Canadian Journal of Anesthesia*, 67. DOI:10.1007/s12630-020-01770-w
- Strasser, B. J., & Schlich, T. (2020). A History Of The Medical Mask And The Rise Of Throwaway Culture. *The Lancet*, 396(10243), 19–20. DOI:10.1016/S0140-6736(20)31207-1
- Tanisali, G., Sozak, A., Bulut, A. S., Sander, T. Z., Dogan, O., Dağ, Ç., Gönen, M., Can, F., DeMirici, H., & Ergonul, O. (2021). Effectiveness Of Different Types Of Mask In Aerosol Dispersion In SARS-CoV-2 Infection. *International Journal of Infectious Diseases*, 109, 310–314. DOI:10.1016/j.ijid.2021.06.029
- Tavernini, S., Church, T. K., Lewis, D. A., Noga, M., Martin, A. R., & Finlay, W. H. (2018).

- Deposition Of Micrometer-sized Aerosol Particles In Neonatal Nasal Airway Replicas. *Aerosol Science and Technology*, 52(4), 407–419. DOI:10.1080/02786826.2017.1413489
- Tcharkhtchi, A., Abbasnezhad, N., Zarbini Seydani, M., Zirak, N., Farzaneh, S., & Shirinbayan, M. (2021). An Overview Of Filtration Efficiency Through The Masks: Mechanisms Of The Aerosols Penetration. *Bioactive Materials*, 6(1), 106–122. DOI:10.1016/j.bioactmat.2020.08.002
- The US Public Health Service. (2012). *PART 84 — APPROVAL OF RESPIRATORY PROTECTIVE DEVICES Subpart A — General Provisions Subpart B — Application For Approval Subpart E — Quality Control*.
- U.S. Environmental Protection Agency (EPA). (2009). *Metabolically Derived Human Ventilation Rates: A Revised Approach Based Upon Oxygen Consumption Rates*.
- Villani, A., Bozzola, E., Staiano, A., Agostiniani, R., Del Vecchio, A., Zamperini, N., Marino, F., Vecchio, D., & Corsello, G. (2020). Facial Masks In Children: The Position Statement Of The Italian Pediatric Society. *Italian Journal of Pediatrics*, 46(1), 1–2. DOI:10.1186/s13052-020-00898-1
- Viscusi, D. J., Bergman, M. S., Novak, D. A., Faulkner, K. A., Palmiero, A., Powell, J., & Shaffer, R. E. (2011). Impact Of Three Biological Decontamination Methods On Filtering Facepiece Respirator Fit, Odor, Comfort, And Donning Ease. *Journal of Occupational and Environmental Hygiene*, 8(7), 426–436. DOI:10.1080/15459624.2011.585927
- Viscusi, D. J., Bergman, M., Sinkule, E., & Shaffer, R. E. (2009). Evaluation Of The Filtration Performance Of 21 N95 Filtering Face Piece Respirators After Prolonged Storage. *American Journal of Infection Control*, 37(5), 381–386. DOI:10.1016/j.ajic.2008.09.021
- Viscusi, D. J., King, W. P., & Shaffer, R. E. (2007). Effect Of Decontamination On The Filtration

- Efficiency Of Two Filtering Facepiece Respirator Models. *International Society for Respiratory Protection*, 24, 93–107.
- WHO. (2020). *Advice On The Use Of Masks In The Context Of COVID-19: Interim Guidance*. WHO. [https://apps.who.int/iris/bitstream/handle/10665/332293/WHO-2019-nCov-IPC\\_Masks-2020.4-eng.pdf?sequence=1&isAllowed=y](https://apps.who.int/iris/bitstream/handle/10665/332293/WHO-2019-nCov-IPC_Masks-2020.4-eng.pdf?sequence=1&isAllowed=y) . Accessed January 4, 2021.
- Xi, J., Berlinski, A., Zhou, Y., Greenberg, B., & Ou, X. (2012). Breathing Resistance And Ultrafine Particle Deposition In Nasal-laryngeal Airways Of A Newborn, An Infant, A Child, And An Adult. *Annals of Biomedical Engineering*, 40(12), 2579–2595. DOI:10.1007/s10439-012-0603-7
- Xing, Y. F., Xu, Y. H., Shi, M. H., & Lian, Y. X. (2016). The Impact Of PM<sub>2.5</sub> On The Human Respiratory System. *Journal of Thoracic Disease*, 8(1), E69–E74. DOI:10.3978/j.issn.2072-1439.2016.01.19
- Xu, J., Xiao, X., Zhang, W., Xu, R., Kim, S. C., Cui, Y., Howard, T. T., & Wu, E. (2020). Air-Filtering Masks For Respiratory Protection From PM<sub>2.5</sub> And Pandemic Pathogens. *One Earth*, 3(5), 574–589. DOI:10.1016/j.oneear.2020.10.014
- Zangmeister, C. D., Radney, J. G., Vicenzi, E. P., & Weaver, J. L. (2020). Filtration Efficiencies Of Nanoscale Aerosol By Cloth Mask Materials Used To Slow The Spread Of SARS-CoV-2. *ACS Nano*, 14(7), 9188–9200. DOI:10.1021/acsnano.0c05025
- Zhou, S. S., Lukula, S., Chiossone, C., Nims, R. W., Suchmann, D. B., & Ijaz, M. K. (2018). Assessment Of A Respiratory Face Mask For Capturing Air Pollutants And Pathogens Including Human Influenza And Rhinoviruses. *Journal of Thoracic Disease*, 10(3), 2059–2069. DOI:10.21037/jtd.2018.03.103